

Testing of Stator Windings for Thermal Aging

Final Report

Technical Report

Testing of Stator Windings for Thermal Aging

Final Report

1009252

Final Report, December 2003

EPRI Project Manager
J. Stein

DISCLAIMER OF WARRANTIES AND LIMITATION OF LIABILITIES

THIS DOCUMENT WAS PREPARED BY THE ORGANIZATION(S) NAMED BELOW AS AN ACCOUNT OF WORK SPONSORED OR COSPONSORED BY THE ELECTRIC POWER RESEARCH INSTITUTE, INC. (EPRI). NEITHER EPRI, ANY MEMBER OF EPRI, ANY COSPONSOR, THE ORGANIZATION(S) BELOW, NOR ANY PERSON ACTING ON BEHALF OF ANY OF THEM:

(A) MAKES ANY WARRANTY OR REPRESENTATION WHATSOEVER, EXPRESS OR IMPLIED, (I) WITH RESPECT TO THE USE OF ANY INFORMATION, APPARATUS, METHOD, PROCESS, OR SIMILAR ITEM DISCLOSED IN THIS DOCUMENT, INCLUDING MERCHANTABILITY AND FITNESS FOR A PARTICULAR PURPOSE, OR (II) THAT SUCH USE DOES NOT INFRINGE ON OR INTERFERE WITH PRIVATELY OWNED RIGHTS, INCLUDING ANY PARTY'S INTELLECTUAL PROPERTY, OR (III) THAT THIS DOCUMENT IS SUITABLE TO ANY PARTICULAR USER'S CIRCUMSTANCE; OR

(B) ASSUMES RESPONSIBILITY FOR ANY DAMAGES OR OTHER LIABILITY WHATSOEVER (INCLUDING ANY CONSEQUENTIAL DAMAGES, EVEN IF EPRI OR ANY EPRI REPRESENTATIVE HAS BEEN ADVISED OF THE POSSIBILITY OF SUCH DAMAGES) RESULTING FROM YOUR SELECTION OR USE OF THIS DOCUMENT OR ANY INFORMATION, APPARATUS, METHOD, PROCESS, OR SIMILAR ITEM DISCLOSED IN THIS DOCUMENT.

ORGANIZATION(S) THAT PREPARED THIS DOCUMENT

Kinectrics Inc.

ORDERING INFORMATION

Requests for copies of this report should be directed to EPRI Orders and Conferences, 1355 Willow Way, Suite 278, Concord, CA 94520, (800) 313-3774, press 2 or internally x5379, (925) 609-9169, (925) 609-1310 (fax).

Electric Power Research Institute and EPRI are registered service marks of the Electric Power Research Institute, Inc. EPRI. ELECTRIFY THE WORLD is a service mark of the Electric Power Research Institute, Inc.

Copyright © 2003 Electric Power Research Institute, Inc. All rights reserved.

CITATIONS

This report was prepared by

Kinectrics Inc.
800 Kipling Avenue
Toronto, ON, Canada M8Z 6C4

Principal Investigators

J. Braun
H. Sedding

This report describes research sponsored by EPRI.

The report is a corporate document that should be cited in the literature in the following manner:

Testing of Stator Windings for Thermal Aging: Final Report, EPRI, Palo Alto, CA: 2003.
1009252.

PRODUCT DESCRIPTION

Electrical insulation used in stator and rotor windings, as well as core laminations, has a major impact on the reliability of large motors and generators. Insulation failure, directly or indirectly, will result in machine failure, which in turn causes forced outages, reduced reliability, and increased maintenance and repair costs. Since many insulation failures originate with aging, which occurs over many years, insulation failure rates will increase in older equipment. Thus, electrical insulation will often determine a machine's remaining useful life, a correlation important to asset management programs. This project's goal is to establish the feasibility of correlating thermal aging of stator coil/bar insulation to dielectric changes measured at frequencies other than 60 Hz.

Results & Findings

Generally, all the diagnostic tests, with one significant exception, correlated with each other and the dimensional measurements of the bars pre- and post-aging. However, return-voltage measurement (RVM) results could not be interpreted and did not seem to behave linearly with aging. Although RVM testing results were disappointing, this situation could be improved by more fundamental work on applying this technique to mica-filled materials.

More encouraging results were obtained from low-frequency dielectric spectroscopy, which produced results consistent with conventional power frequency diagnostic methods. However, the purpose of using low-frequency dielectric spectroscopy is to augment existing diagnostics, specifically to detect at an early stage the onset of thermal deterioration. Thus, while this low-frequency technique appears promising, more work is needed to determine that the test is capable of accurately characterizing low-level thermal damage.

Challenges & Objectives

Pressures on utilities to operate more efficiently, minimize unnecessary maintenance costs, and accurately estimate a component's remaining life have created a need to effectively assess insulation condition. Of special interest are tests or monitors that can help assess insulation condition while machines are operating normally. Manufacturers, consultants, and utilities are all working to improve their ability to assess rotating machine insulation condition.

Applications, Values & Use

The physical properties of stator insulation change with thermal aging. Typical insulation characterization techniques include tensile strength and elongation, dynamic mechanical analysis (DMA), differential scanning calorimetry (DSC), oxidation induction time (OIT), oxidation induction temperature, Fourier transform infrared spectroscopy (FTIR), gel content, swelling ratio, density, and glass-transition temperature. However, all these techniques, though very powerful, are destructive and cannot be used for *in-situ* tests of stator insulation.

EPRI Perspective

Utilities use many *in-situ* tests and monitors to determine the condition of stator, rotor, and coreplate insulation systems in motors and generators. Most of these methods are off-line tests that are done with the machine out of service. The most widely used tests are a dc or ac high-potential (hipot) test (EPRI report 1000666, *Guideline for Rotating Electrical Machine Hipot Testing*), together with an insulation resistance (IR) and polarization index (PI, ratio of IR at ten and one minute) test. Some utilities augment this information with partial discharge (PD), dissipation factor, dissipation factor tip-up, and/or capacitance tests. However, these tests provide little, if any, information on thermal aging of the insulation system. This project is an extension of work published in 2000 and 2002 (EPRI report 1000376, *Testing of Stator Winding for Thermal Aging*).

Approach

The project team removed high-voltage stator bars from a hydraulic generator and subjected them to thermal aging at a temperature of 145°C for 2700 hours to accelerate the effects of thermal stress on the insulation system. The team took two steps to ensure satisfactory aging: (1) they used oxygen-enriched air and (2) periodically measured oxygen concentration in the outflow from the specialized test cell. With a measured oxygen index of 28.9%, an upper limit of 25% oxygen by volume in the test chamber was set. All bars were subjected to a one-minute insulation resistance test as well as standard power frequency PD, capacitance, and dissipation factor tests prior to, and following, the thermal-aging program. The team also used non-60-Hz techniques. These techniques included low-frequency dielectric spectroscopy, RVM, and high-voltage DC ramp.

Keywords

Rotating machine
Stator
Thermal aging
Diagnostic

ABSTRACT

The electrical insulation used in stator windings, as well as core laminations, has a major impact on the reliability of large motors and generators. Thermal aging of the insulation, especially in conjunction with the differential expansion forces experienced by conductor and insulation, can lead to a progressive embrittlement of the electrical insulation. The objective of the present project is to establish the feasibility of correlating thermal aging of stator coil/bar insulation to dielectric changes measured at frequencies other than 60Hz. High-voltage stator bars, removed from a hydraulic generator, were subjected to thermal aging at a temperature of +145°C for 2700 hours to accelerate the effects of thermal stress on the insulation system. Two steps were taken to ensure satisfactory aging: 1) the use of oxygen enriched air and 2) the periodic measurement of oxygen concentration in the outflow from the specialized test cell. With a measured oxygen index of 28.9%, an upper limit of 25% oxygen by volume in the test chamber was set. All bars were subjected to a one-minute insulation-resistance test and standard power-frequency PD, capacitance, and dissipation factor tests prior to and following the thermal-aging program. Additionally, non-60Hz techniques were used. They included low-frequency dielectric spectroscopy, return-voltage measurement (RVM), and high-voltage DC ramp.

The results of the project demonstrated that the artificial aging method employed was valid. Results of diagnostic testing, both conventional and non-power frequency, verified the occurrence of additional degradation of the service-aged insulation. While low-frequency dielectric spectroscopy showed promising results as a means to determine early onset of thermal aging, the RVM technique requires significant fundamental efforts before implementation as a reliable diagnostic can be contemplated.

CONTENTS

- 1 INTRODUCTION 1-1**
- 2 SELECTION OF SUITABLE STATOR BARS 2-1**
- 3 INITIAL CHARACTERIZATION AND AGING OF STATOR BARS 3-1**
- 4 DIAGNOSTIC CHARACTERIZATION 4-1**
 - 4.1 Test Results - Conventional Diagnostics 4-3
 - 4.2 Dimensional Measurements 4-12
 - 4.3 Dielectric Spectroscopy Test Results 4-14
 - 4.3.1 Dielectric Spectroscopy Results – Prior to Aging 4-14
 - 4.3.2 Dielectric Spectroscopy Results – After Aging 4-20
 - 4.4 Return Voltage Measurement Results 4-27
 - 4.5 Summary of Dielectric Response Results 4-39
- 5 CONCLUSIONS 5-1**
- 6 FURTHER WORK 6-1**
- 7 REFERENCES 7-1**

LIST OF FIGURES

Figure 3-1 Bars loaded into aging cell	3-2
Figure 4-1 View of aging cell with gas handling and temperature control equipment.....	4-2
Figure 4-2 Comparison of DIV values, pre- and post-aging	4-6
Figure 4-3 Comparison of DEV values, pre- and post-aging.....	4-6
Figure 4-4 Comparison of positive PD magnitude values, pre- and post-aging	4-7
Figure 4-5 Comparison of negative PD magnitude values, pre- and post-aging	4-7
Figure 4-6 Comparison of ΔC values, pre- and post-aging	4-10
Figure 4-7 Comparison of tip-up values, pre- and post-aging	4-10
Figure 4-8 Comparison of capacitance values, pre- and post-aging	4-11
Figure 4-9 Comparison of dissipation factor values, pre- and post-aging	4-11
Figure 4-10 Dielectric response of bar T5, control bar	4-15
Figure 4-11 Dielectric response of bar T29, pre-aging.....	4-15
Figure 4-12 Dielectric response of bar T42, pre-aging.....	4-16
Figure 4-13 Dielectric response of bar T218, pre-aging.....	4-16
Figure 4-14 Dielectric response of bar T321, pre-aging.....	4-17
Figure 4-15 Dielectric response of bar B378, pre-aging	4-17
Figure 4-16 Dielectric response of bar T386, pre-aging.....	4-18
Figure 4-17 Dielectric response of bar B239, pre-aging	4-18
Figure 4-18 Dielectric response of bar B246, pre-aging	4-19
Figure 4-19 Dielectric response of bar T402, pre-aging.....	4-19
Figure 4-20 Dielectric response of bar B445, pre-aging	4-20
Figure 4-21 Dielectric response of bar T5, control bar.....	4-22
Figure 4-22 Dielectric response of bar T29, post-aging	4-22
Figure 4-23 Dielectric response of bar T42, post-aging	4-23
Figure 4-24 Dielectric response of bar T218, post-aging	4-23
Figure 4-25 Dielectric response of bar B239, post-aging.....	4-24
Figure 4-26 Dielectric response of bar B246, post-aging.....	4-24
Figure 4-27 Dielectric response of bar B321, post-aging.....	4-25
Figure 4-28 Dielectric response of bar B378, post-aging.....	4-25
Figure 4-29 Dielectric response of bar T386, post-aging	4-26
Figure 4-30 Dielectric response of bar T402, post-aging	4-26

Figure 4-31 Dielectric response of bar B445, post-aging	4-27
Figure 4-32 RVM response of bar T5, control bar	4-28
Figure 4-33 RVM response of bar T29, pre-aging	4-29
Figure 4-34 RVM response of bar T42, pre-aging	4-29
Figure 4-35 RVM response of bar T218, pre-aging	4-30
Figure 4-36 RVM response of bar T321, pre-aging	4-30
Figure 4-37 RVM response of bar B378, pre-aging	4-31
Figure 4-38 RVM response of bar T386, pre-aging	4-31
Figure 4-39 RVM response of bar B239, pre-aging	4-32
Figure 4-40 RVM response of bar B246, pre-aging	4-32
Figure 4-41 RVM response of bar T402, pre-aging	4-33
Figure 4-42 RVM response of bar B445, pre-aging	4-33
Figure 4-43 RVM response of bar T5, control bar	4-34
Figure 4-44 RVM response of bar T29, post-aging.....	4-34
Figure 4-45 RVM response of bar T42, post-aging.....	4-35
Figure 4-46 RVM response of bar T218, post-aging.....	4-35
Figure 4-47 RVM response of bar T321, post-aging.....	4-36
Figure 4-48 RVM response of bar B378, post-aging	4-36
Figure 4-49 RVM response of bar T386, post-aging.....	4-37
Figure 4-50 RVM response of bar B239, post-aging	4-37
Figure 4-51 RVM response of bar B246, post-aging	4-38
Figure 4-52 RVM response of bar T402, post-aging.....	4-38
Figure 4-53 RVM response of bar B445, post-aging	4-39

LIST OF TABLES

Table 4-1 Insulation resistance results, before and after aging.....	4-3
Table 4-2 Partial discharge results, as received.....	4-4
Table 4-3 PD results after thermal aging.....	4-5
Table 4-4 Capacitance and dissipation factor results, as received.....	4-8
Table 4-5 Capacitance and dissipation factor results, post-aging.....	4-9
Table 4-6 Dimensional measurements of bars, pre-aging.....	4-13
Table 4-7 Dimensional measurements of bars, post-aging.....	4-13
Table 4-8 Comparison of $\tan \delta$ of aged and unaged bars at two frequencies.....	4-21
Table 4-9 Comparison of tip-up of aged and unaged bars at two frequencies.....	4-21
Table 4-10 Comparison of RVM results before and after aging.....	4-28
Table 5-1 Summary of correlation of diagnostic results with respect to bar condition.....	5-2

1

INTRODUCTION

The electrical insulation used in stator and rotor windings, as well as core laminations, has a major impact on the reliability of large motors and generators. Failure of the insulation directly or indirectly will result in failure of the machine, which in turn causes forced outages, reduced reliability and increased maintenance and repair costs. Industry surveys have shown that insulation problems are a predominant cause of motor and generator failure [1,2]. Since many insulation failures originate with aging that occurs over many years, insulation failure rates will increase in older equipment, and thus the electrical insulation will often determine the remaining useful life of a machine. This latter aspect is important in asset management programs to establish current condition.

Pressures on utilities to operate more efficiently, and in particular to minimize unnecessary maintenance costs, together with the need to determine the remaining life of components, have created a need to develop means for assessing insulation condition. Of special interest are tests or monitors that can aid in the assessment of insulation condition while the machine is operating normally. Manufacturers, consultants and utilities are all trying to improve their ability to assess rotating machine insulation condition.

The machine environment creates several mechanisms that can age stator insulation. In addition to electrical and mechanical stresses, heating of the insulation due to I^2R losses in the conductor is an important thermal aging factor, especially in conjunction with the differential expansion forces experienced by conductor and insulation, leading to a progressive degradation of the electrical insulation. Thermal aging will result in an initial hardening - which may even be beneficial to the insulation performance - followed by gradual embrittlement of the insulation. Diagnostic testing is intended to detect the progressive deterioration of the insulation system.

As well, insulation system deterioration by thermal cycling will result from the different coefficients of expansion of copper and insulation. Also, since the primary heat source in a winding is the losses in the copper, the copper reaches a higher temperature more rapidly than the surrounding insulation. The result is that when a machine is quickly raised to full load, the copper expands in the axial direction much more quickly than the insulation. Even if the groundwall insulation were free to move with respect to the stator core, a mechanical shear stress is created between the copper and the groundwall insulation, and within the groundwall insulation. Depending on the length of the slot section and the cohesive strength of the insulation, the bond to the copper may be broken and/or the insulation may delaminate. Significant debonding or delamination creates air gaps in the insulation, leading to partial discharges which erode the insulation. Alternatively, debonding, together with the 120 Hz magnetic forces, gradually allow the strand conductors to move relative to one another, resulting in abrasion of the strand insulation and strand shorts. Over several years and hundreds of rapid load cycles, the insulation eventually fails.

The physical properties of stator insulation are known to change with thermal aging. Typical insulation characterization techniques include tensile strength & elongation, dynamic mechanical analysis (DMA), differential scanning calorimetry (DSC), oxidation induction time (OIT), oxidation induction temperature, Fourier transform infrared spectroscopy (FTIR), gel content, swelling ratio, density and glass transition temperature. However, all the above techniques, though very powerful, are destructive and cannot be used for in-situ tests of stator insulation.

Many in-situ tests and monitors are presently used by utilities to determine the condition of the stator, rotor and coreplate insulation systems used in motors and generators. Most of these methods are off-line tests which are done with the machine out of service. The most widely used tests are a dc or ac high potential (hipot) test, together with an insulation resistance (IR) and polarization index (PI, ratio of IR at ten and one minute) test. Some utilities augment this information with partial discharge (PD), dissipation factor, dissipation factor tip-up, and/or capacitance tests. However, these tests provide little, if any, information on thermal aging of the insulation system.

Earlier studies on aged cable insulations underlined the value of performing tests at other than power frequency and/or dc. DC insulation resistance and the related polarization index were found to be insensitive to thermal aging for typical cable insulation (SBR, PVC, butyl, PE and EPR), even in a very advanced state of deterioration. The dielectric characteristics studied over a broad range of frequencies, and expressed for instance as tan delta, show variations of dielectric properties, as a function of frequency, with the type of cable insulation.

The objective of the present project is to establish the feasibility of correlating thermal aging of stator coil/bar insulation to dielectric changes measured at frequencies other than 60Hz.

2

SELECTION OF SUITABLE STATOR BARS

In order to fulfill the objectives of the project, a sufficiently large number of stator bars were required. Among the criteria considered when selecting suitable test objects were,

- Cost
- Materials
- Machine type
- Availability

Costs associated with manufacturing stator bars specifically for this project would have been prohibitive, e.g., a single bar for a direct liquid-cooled winding can cost in the range of \$80,000. Consequently, a request for appropriate samples was sent to EPRI member utilities. This request was for stator bars or coils from large generators, insulated with materials typical of those found in present common use. Older, asphaltic-mica systems, although still encountered on operating machines, were precluded from the study. Consequently, stator windings insulated with thermoset materials, i.e., those in which the binder was an epoxy or polyester resin, were sought. After a lengthy search period, stator bars insulated with a modern epoxy-mica insulation system were obtained.

A total of 12 service-aged stator bars were donated to the project by Consumers Energy from a plant equipped with six motor/generator sets with a nominal rating of 20 kV, 388 MVA. The bars are of the Roebel type with groundwall insulation composed of large flake mica and a fibre glass backing tape. Consolidation of the insulation is achieved using an epoxy resin. The sample population of bars consists of eight tops and four bottoms. Each bar has a total length of 3.10 m, of which the slot cell comprises 2.15 m. Visual inspection of the bars showed that they were in good condition considering the service history.

3

INITIAL CHARACTERIZATION AND AGING OF STATOR BARS

An accelerated aging test is intended to compare objectively the long term performance of insulation systems. In an accelerated aging test, one or more stresses believed to contribute to aging are applied to the insulation system at significantly higher levels than those experienced in normal service. Under enhanced stresses the degradation of insulation occurs in hours, days or weeks rather than years. Bars with different insulation systems are subjected to specified enhanced stresses for a fixed period. The levels and duration of stresses applied in the test should preferably be based on the functional specification of the insulation system. The insulation system suffering less degradation in such a test is relatively the better insulation system.

Several North American utilities have been qualifying insulation systems, and hence sources of supply, on the basis of a voltage endurance test. In this test, the capability of full size stator coils or bars is assessed by energizing the coils at a prescribed voltage at elevated temperature. The pass/fail criterion is based on whether the coil/bar survived the test for a predetermined time period. As well, some utilities have applied a thermal cycling test to stator coils and bars from machines subject to such stresses. This test is performed on full size stator bars and coils and provides valuable data on the ability of the groundwall insulation to resist delamination and remain well bonded to the copper stack.

The principal aging stress under consideration in this study is thermal, consequently, consideration was given to various thermal aging methods. In principle, the simplest thermal aging method is to place the bars in an oven and heat them at a fixed, elevated temperature for a prescribed time. However, the size of the test objects, approximately 2.5 m in length, presents a practical problem. Ovens of sufficient size were not available at Kinectrics facilities. Alternatively, heater plates can be applied to the slot portion of the bar. This method is used in voltage endurance tests [3,4] of stator coils or bars. Applying heat in this way produces a thermal gradient across the groundwall insulation, albeit in the opposite sense from that encountered in service, i.e., the gradient is driven from the outside in rather than inside out. This method of aging the stator bars was selected for this study.

A specialized test facility has been designed to keep the bars under high temperatures while simultaneously exposing them to oxygen enriched air. Thermal aging results in the rapid consumption of oxygen in the air surrounding the bars; if care is not taken, oxygen depletion can be such that little thermal aging is taking place. Two steps are taken to ensure satisfactory oxygen availability during the aging experiment, the use of oxygen enriched air and the periodic measurement of oxygen concentration in the outflow from the specialized test cell. To control the aging atmosphere, the test cell was designed as an air-tight enclosure. Prior to commencing

thermal aging using this method, the oxygen index of the epoxy-mica insulation was determined to avoid potential problems if the combustion limit of the test set up was exceeded. The index was found, by measurement, to be 28.9%; thus an upper limit of 25% oxygen by volume in the test chamber was set. This value is approximately 4% higher in oxygen content than normal atmosphere. The bars were aged in this enriched oxygen environment at a temperature of 145 C for 2700 hours.

Following initial (conventional) characterization the stator bars were subjected to accelerated thermal aging, nominally to failure (as defined by the diagnostic tests), by the method described above. Figures 3-1 and 4-1 illustrate the configuration of the bars and the aging cell.



Figure 3-1
Bars loaded into aging cell

4

DIAGNOSTIC CHARACTERIZATION

Diagnostic characterization of stator bars included conventional and novel testing through the aging period. Novel techniques included low frequency dielectric spectroscopy, return voltage measurement (RVM) and high voltage dc ramp.

The well-established techniques include:

- Insulation resistance
- Dissipation (power) factor tip-up
- Partial discharge

Partial discharge (PD) data provides information on the void size and distribution of a stator bar or coil. The voids result either from improper impregnation and cure during manufacturing or from delamination of the groundwall insulation in service. A typical PD test consists of measuring the PD magnitude at a prescribed voltage, typically the nominal line-to-ground voltage of the machine, as well as the discharge inception and extinction voltage, DIV and DEV respectively. Proper analysis and interpretation of these parameters can provide insight into the location, as well as size, of the voids.



Figure 4-1
View of aging cell with gas handling and temperature control equipment

Capacitance and dissipation factor tests also provide a measure of void content, however, this is a spatially averaged value, i.e., the test cannot distinguish the contribution of one large defect to that from a multiplicity of smaller voids. This test also provides a measure of the bulk properties of the insulation and can be used to some extent to assess cure. Capacitance and dissipation factor values are recorded at more than one voltage. Usually measurements are made at a voltage below DIV and at the rated line-to-ground voltage of the stator winding. The difference between the two values is known as the dissipation factor tip-up.

Dielectric spectroscopy is a term generically applied to a number of techniques [5-9] in which properties such as capacitance, permittivity, dielectric constant and tangent delta (loss factor) are determined over a range of frequencies typically extending from mHz to kHz. Typically, these methods have been applied to extruded polymers such as those used in cable insulation [6,7]. However, some applications to the investigation of aging in rotating machine insulation have also been reported [9]. The basic properties measured are the same as described above, however, they are recorded at multiple frequencies. Appropriate equipment to perform this measurement

was not available at all times in the project, consequently, data on this technique contained in this report is limited.

4.1 Test Results - Conventional Diagnostics

All of the bars had been removed from the generator and required some preparation prior to performing any testing. Specifically, insulation was removed from each end of the bars to facilitate contact with the copper conductors.

All bars were subjected to a one minute insulation resistance test as well as standard power frequency PD, capacitance and dissipation factor tests prior to, and following, the thermal aging program. The data from these measurements are illustrated in Tables 4-1 to 4-5. Partial discharge measurements were accomplished using a 375 pF coupling capacitor, the output of which is connected, via a power frequency filter, to a 500 MHz bandwidth digital oscilloscope. In addition to measurements of the maximum PD magnitude at 11.5 kV, the discharge inception (DIV) and discharge extinction voltage (DEV) were also recorded. Capacitance and dissipation (power) factor measurements were undertaken using a MultiAmp CB0605 bridge. Values were recorded at 2 and 11.5 kV from which the voltage coefficient (ΔC) and dissipation factor tip-up were calculated. The voltage coefficient is obtained by subtracting the capacitance value at the lower voltage from that at the higher voltage and dividing by the lower voltage capacitance. The resultant is expressed as a percentage. The tip-up is obtained by subtracting the lower voltage dissipation factor from that at the higher voltage.

Table 4-1
Insulation resistance results, before and after aging

Bar	Insulation Resistance (G Ω) Pre-Aging	Insulation Resistance (G Ω) Post-Aging
T5	250	250
T29	225	250
T42	250	250
T218	200	250
T321	200	250
T340	150	250
T386	200	250
T402	300	250
B239	250	250
B246	225	250
B378	200	250
B445	200	250

The insulation resistance data exhibit little change of significance as a function of aging. Both sets of data indicate that the insulation is dry and free of any gross defects such as cracks. This finding is not surprising given the low diagnostic content of the insulation resistance test as well as the nature of the aging method.

Table 4-2
Partial discharge results, as received

Bar	DIV (kV)	DEV (kV)	Max. PD Magnitude (mV)
T5	7.1	6.9	+40/-50
T29	7.0	6.3	+70/-60
T42	4.3	3.6	+200/-200
T218	5.9	5.2	+100/-90
T321	6.3	5.5	+80/-90
T340*	-	-	-
T386	6.7	5.8	+30/-40
T402	6.3	5.7	+50/-40
B239	3.4	2.6	+400/-400
B246	5.6	4.3	+60/-90
B378	5.9	5.5	+100/-120
B445	6.4	5.9	+90/-80

* failed during PD test

Examination of the data in Table 4-2 shows that there are significant differences in the condition of the insulation system of the individual bars. Nominally, bars T5 and T29 exhibit good PD characteristics, i.e., low magnitudes at line-to-ground voltage and relatively high DIV and DEV values. Conversely, bars B239 and T42 with high PD magnitudes and low DIV and DEV levels can be considered as having the highest void content. This variation in PD behaviour may be a function of the electrical position of the bar in the winding thus indicating that electrical aging was the principal deterioration mechanism. However, with no knowledge of the electrical positions of these bars, no such can conclusion can be drawn at this time.

The PD magnitudes, DIV and DEV values following the thermal aging program are recorded in Table 4-3. There are no data for bar T5 which was not subject to thermal aging.

Table 4-3
PD results after thermal aging

Bar	DIV (kV)	DEV (kV)	Max. PD Magnitude (mV)
T5	-	-	-
T29	4.3	3.7	+100/-100
T42	3.8	3.1	+180/-180
T218	5.5	4.8	+320/-380
T321	3.6	2.9	+120/-120
T340*	-	-	-
T386	3.8	3.8	+840/-800
T402	7.1	6.5	+1200/-1050
B239	4.7	4.0	+100/-80
B246	4.3	3.7	+650/-600
B378	5.7	4.9	+380/-240
B445	5.5	4.5	+500/-500

The data contained in Tables 4-2 and 4-3 are summarized graphically in Figures 4-2 through 4-5 to aid comparison of the pre- and post-thermal aging PD results. Closer inspection of Tables 4-2 and 4-3 as well as Figures 4-2 through 4-5 shows that,

1. Significant decreases in DIV and DEV are exhibited by bars T29, T321, T386, B246 and B445 following completion of the aging program.
2. Moderate decreases in DIV and DEV are exhibited by bars T42, T218 and B378.
3. The DIV and DEV values of bars T402 and B239 increased after aging.
4. When the negative PD magnitude data is examined, large increases in PD magnitude are recorded for bars T218, T386, T402, B246 and B445. The data do not show a strong correlation between DIV/DEV and PD magnitude, e.g., the DIV and DEV on bar T218 increase whereas the PD magnitude increases significantly.
5. The largest increase in PD activity was recorded on bar T402.

Overall, the PD data indicate that some of the bars have undergone further delamination as a function of thermal aging. In principle, the lowered DIV and DEV values as well as the higher PD magnitudes observed indicate that void growth and propagation has occurred in the groundwall insulation.

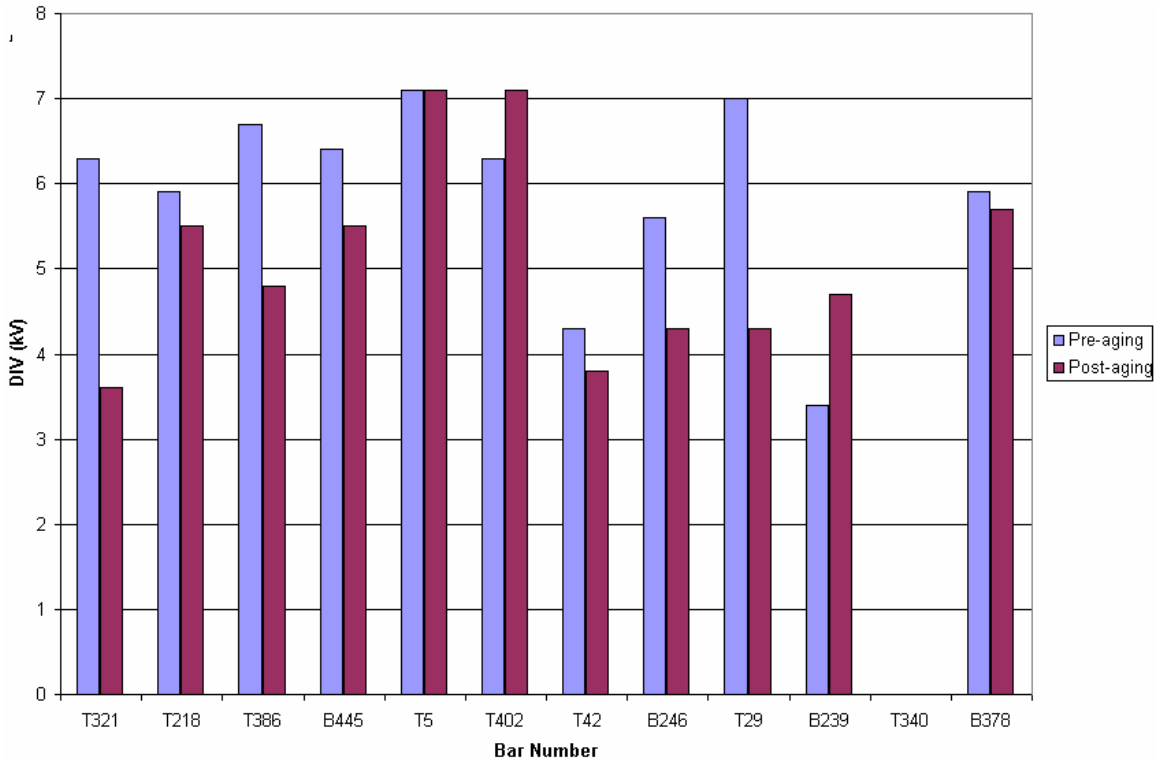


Figure 4-2
Comparison of DIV values, pre- and post-aging

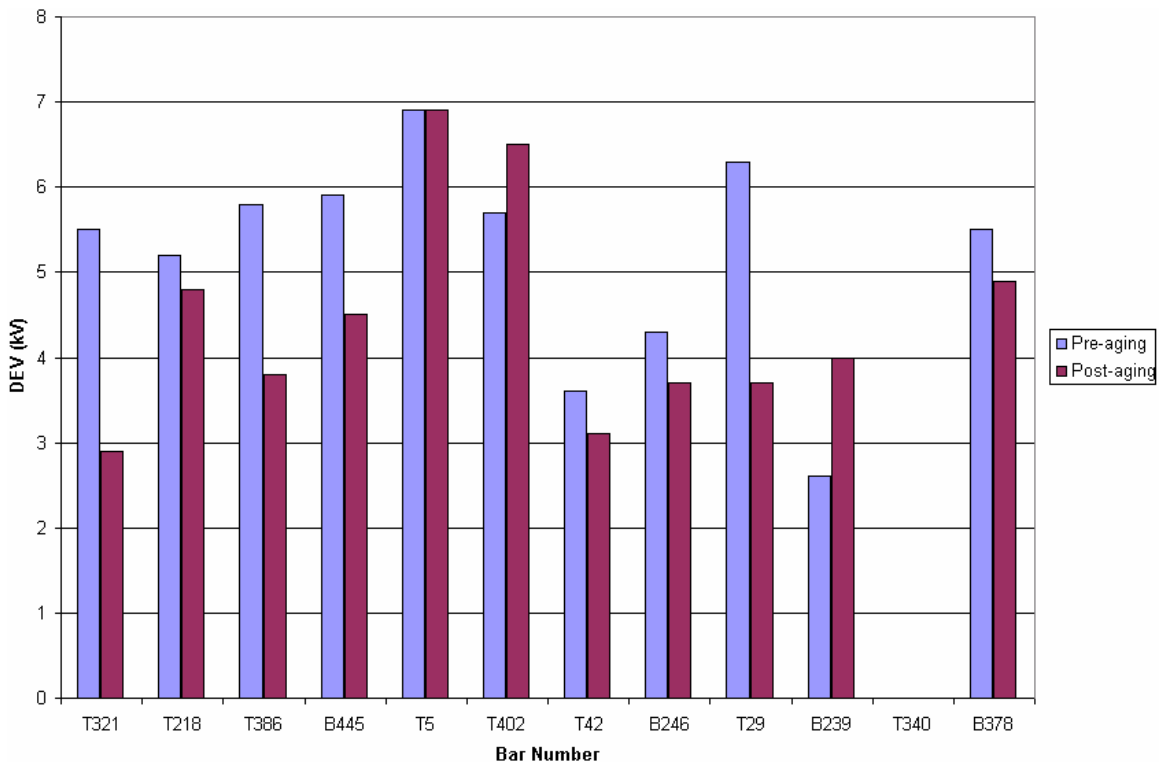


Figure 4-3
Comparison of DEV values, pre- and post-aging

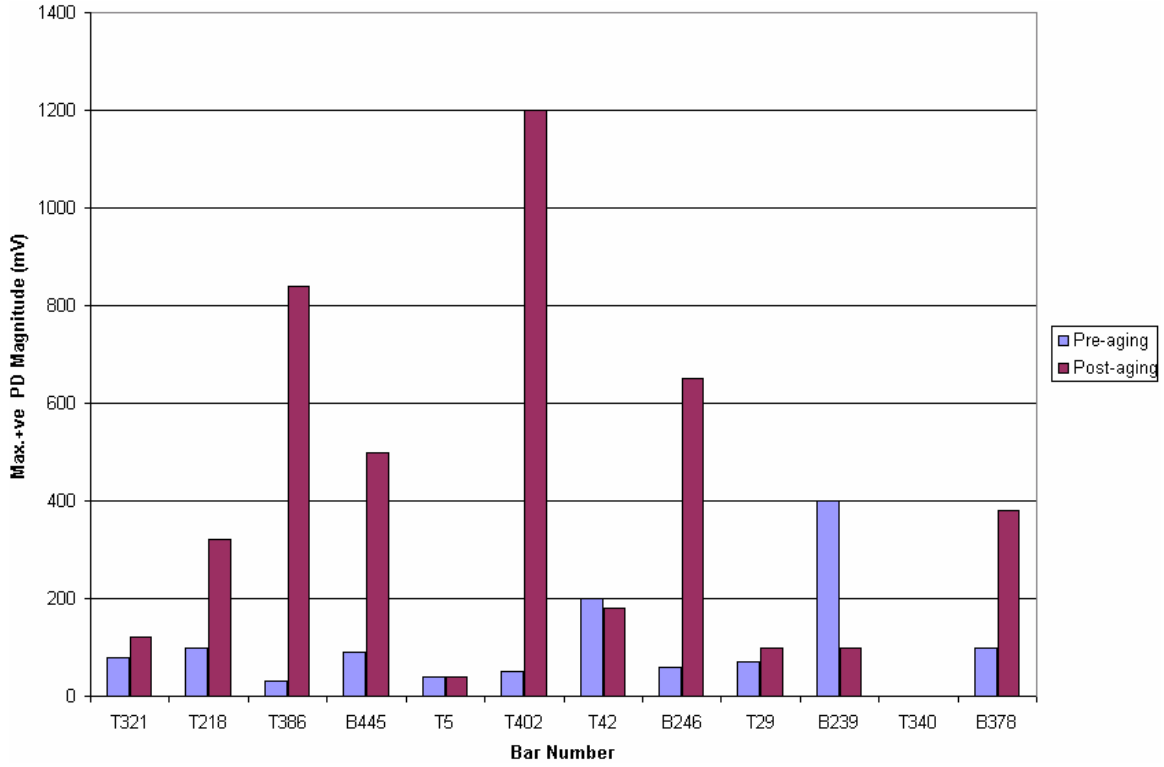


Figure 4-4
Comparison of positive PD magnitude values, pre- and post-aging

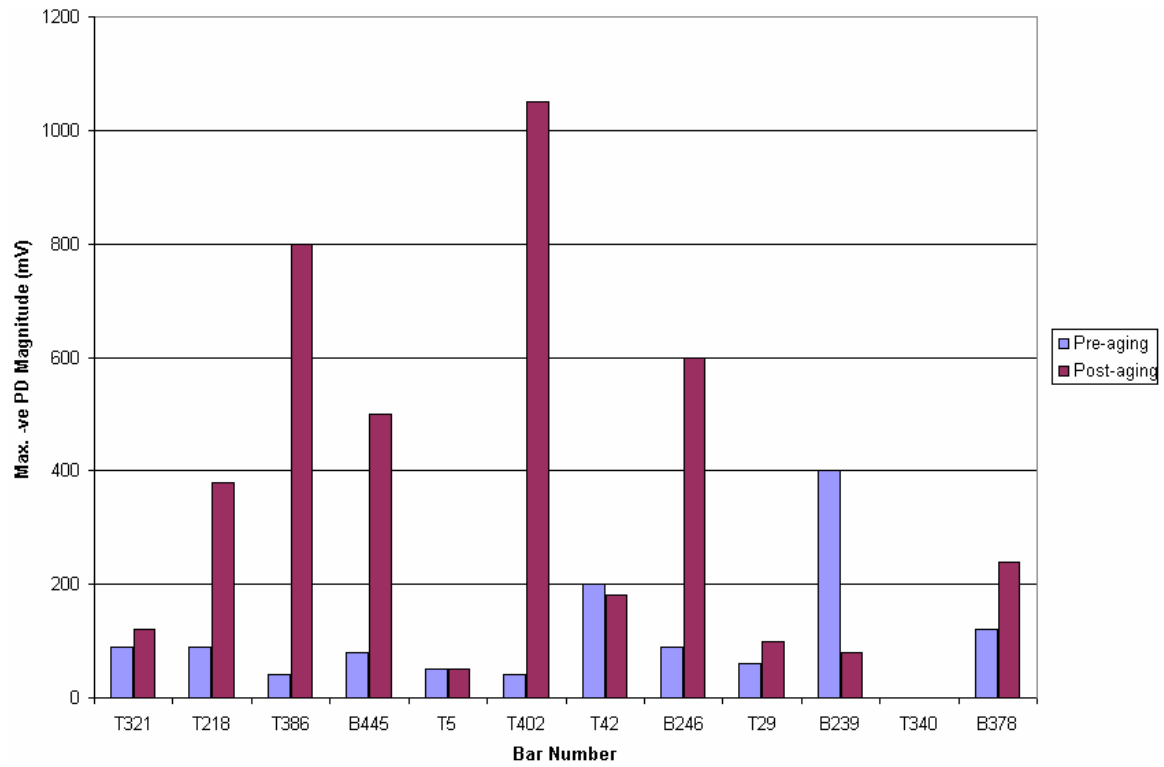


Figure 4-5
Comparison of negative PD magnitude values, pre- and post-aging

Capacitance and dissipation factor were measured using a Multi-Amp CB605 bridge and a 1000 pF standard capacitor. These measurements were performed in broad accordance with IEEE 286 and IEC 894. The stress grading material in the end regions of the bars was not guarded out. Typically efforts are made to minimize the effects of these stress relief coatings, however, the presence of a resistive coating and asbestos in this region mitigated against application of guard electrodes. Consequently, all of the loss measurements reported in this document should be considered carefully because of the nonlinear effects introduced by the stress grading.

Table 4-4
Capacitance and dissipation factor results, as received

Bar	C (nF) @ 2 kV	C (nF) @ 11.5 kV	ΔC (%)	DF (%) @ 2 kV	DF (%) @ 11.5 kV	Tip-Up (%)
T5	3.963	3.990	0.68	1.746	2.327	0.581
T29	4.058	4.086	0.69	2.154	2.732	0.578
T42	3.708	3.772	1.72	2.710	3.504	0.794
T218	3.867	3.917	1.29	2.063	2.907	0.844
T321	3.936	3.979	1.09	2.264	3.090	0.826
T386	4.000	4.026	0.65	1.847	2.295	0.448
T402	3.901	3.928	0.69	2.309	2.847	0.538
B239	3.670	3.733	1.72	1.464	2.110	0.646
B246	3.862	3.907	1.16	2.250	3.004	0.754
B378	3.952	3.985	0.83	2.221	2.948	0.527
B445	3.983	4.028	1.13	2.119	3.049	0.930

Examination of the data in Table 4-4 show that the capacitance and dissipation factor values are consistent with service-aged stator insulation. Typically, both ΔC and tip-up should be below 1%. New stator coils or bars are expected to have tip-up values less than 0.6%, thus the values obtained demonstrate that the bars have undergone some aging during operation. The absolute values of the dissipation factors are higher than normal, however, probably due to the influence of the stress relieving materials in the end arms.

Table 4-5
Capacitance and dissipation factor results, post-aging

Bar	C (nF) @ 2 kV	C (nF) @ 11.5 kV	ΔC (%)	DF (%) @ 2 kV	DF (%) @ 11.5 kV	Tip-Up (%)
T5	3.951	3.974	0.58	1.646	2.103	0.457
T29	3.160	3.178	0.57	2.355	2.970	0.615
T42	2.863	2.878	0.52	1.685	2.136	0.451
T218	3.113	3.136	0.74	1.612	2.306	0.694
T321	3.217	3.245	0.87	1.914	2.670	0.756
T386	2.948	3.025	2.61	1.629	3.508	1.879
T402	2.721	2.795	2.72	2.050	4.674	2.624
B239	2.935	2.967	1.09	1.395	2.290	0.895
B246	2.866	2.910	1.53	1.675	3.205	1.530
B378	2.894	2.926	1.12	2.568	3.730	1.162
B445	2.859	2.908	1.71	1.925	3.550	1.625

Figures 4-6 through 4-9 provide a comparison between the data contained in Tables 4-4 and 4-5.

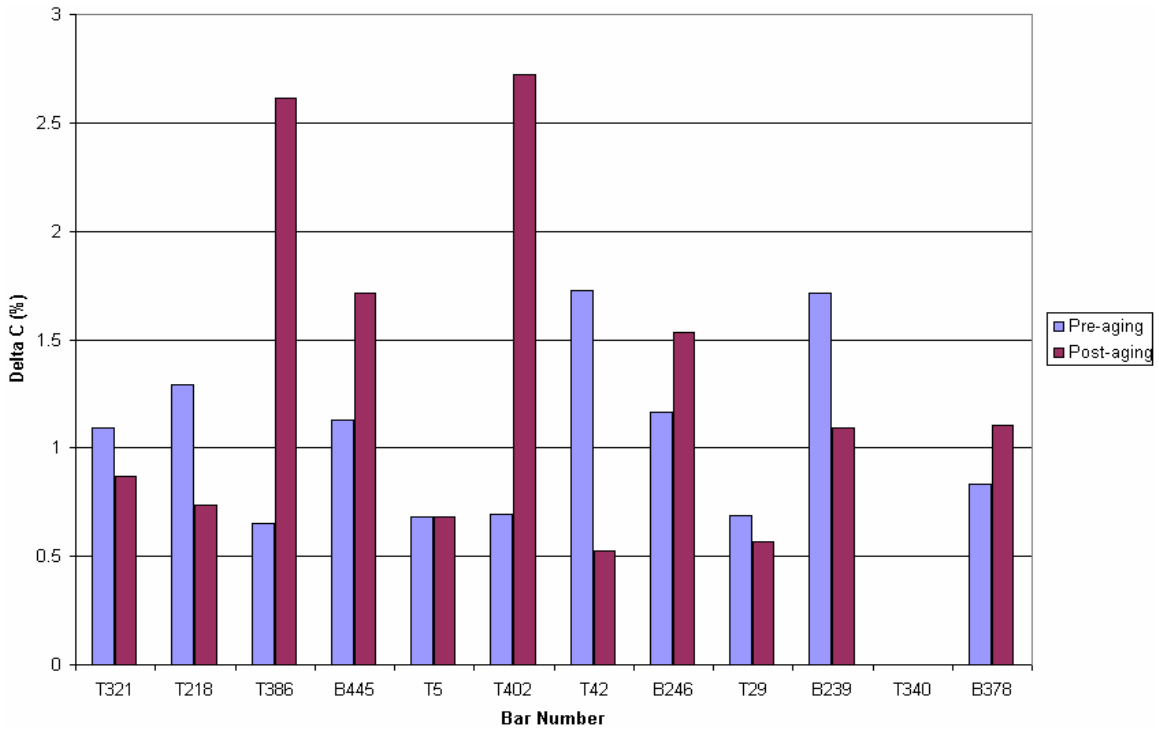


Figure 4-6
Comparison of ΔC values, pre- and post-aging

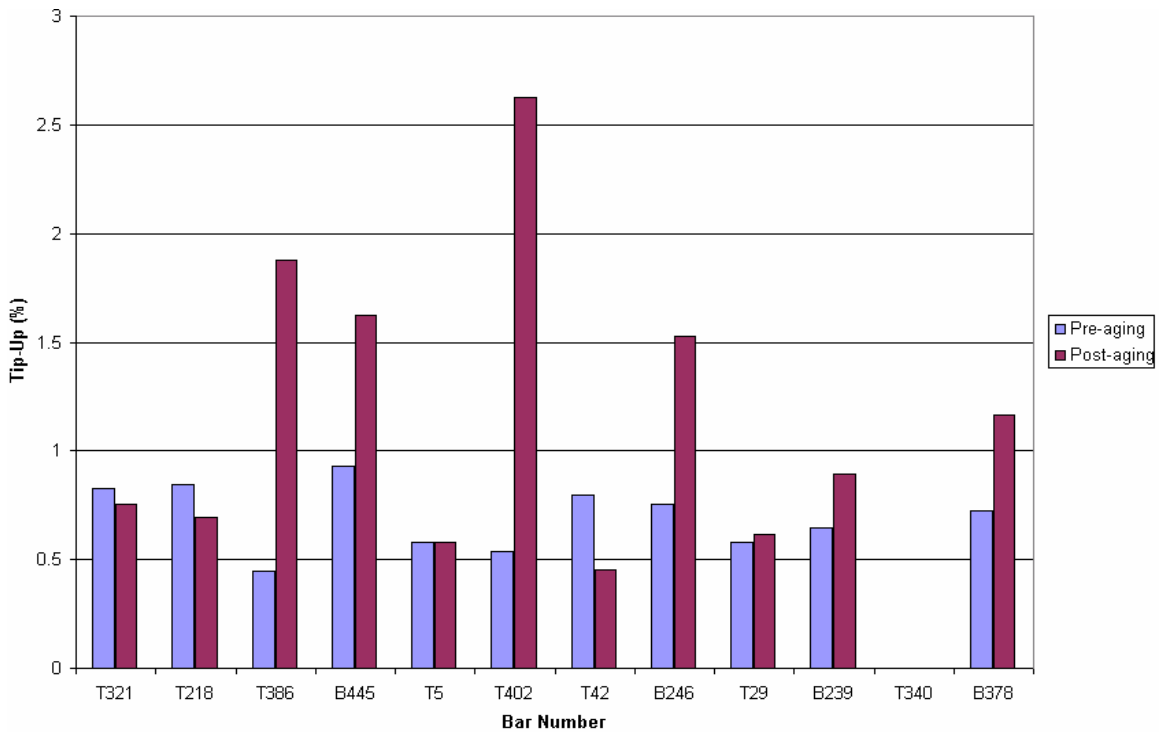


Figure 4-7
Comparison of tip-up values, pre- and post-aging

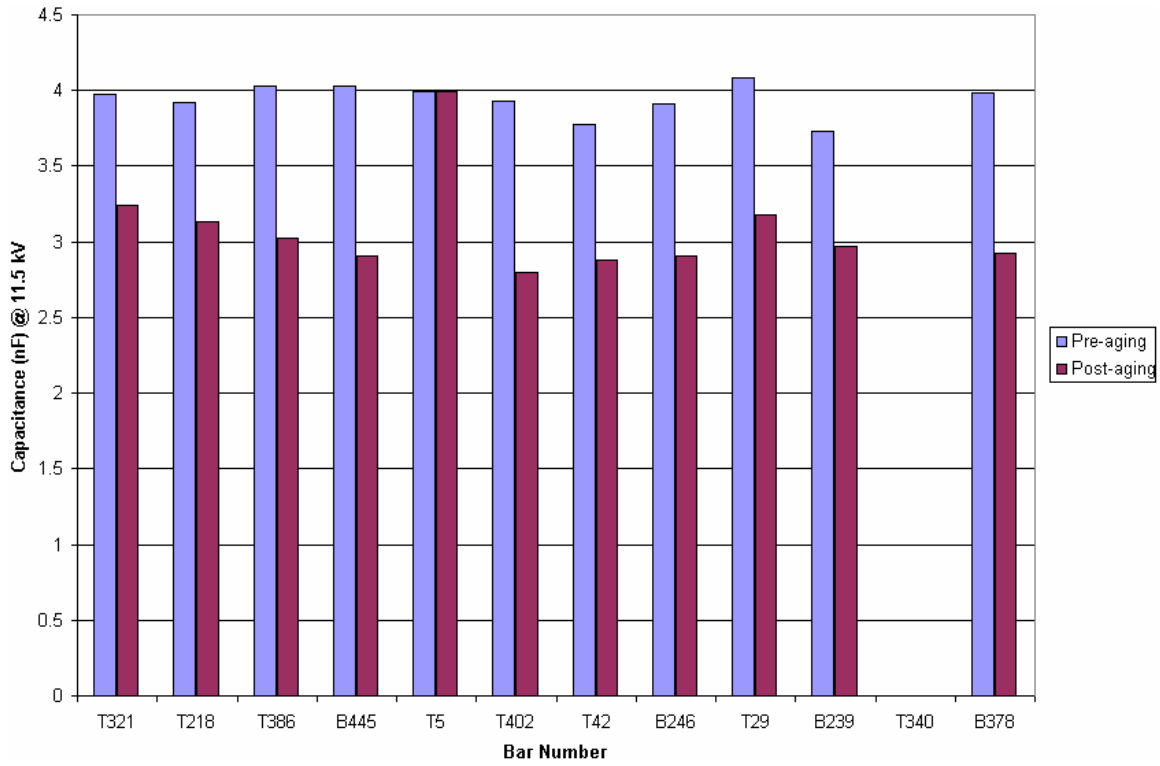


Figure 4-8
Comparison of capacitance values, pre- and post-aging

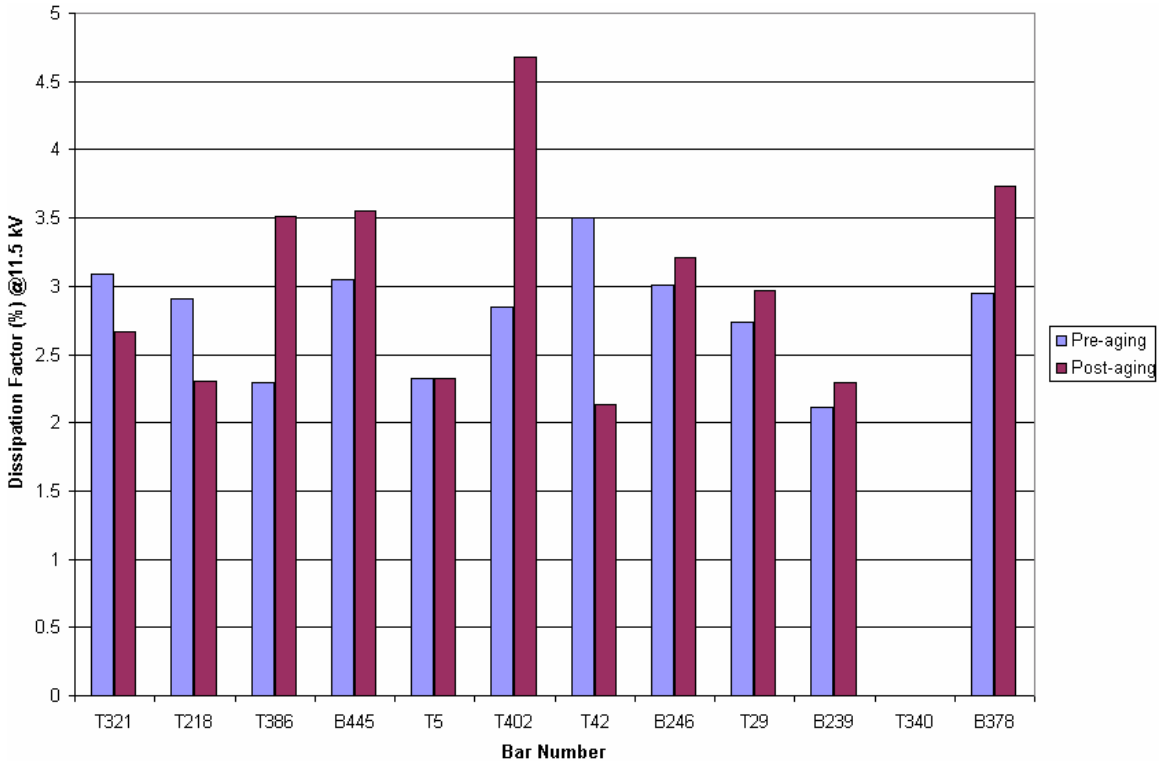


Figure 4-9
Comparison of dissipation factor values, pre- and post-aging

Closer inspection of Tables 4-4 and 4-5 as well as Figures 4-6 through 4-9 shows that,

1. The voltage coefficient, ΔC , and the tip-up values are broadly correlated demonstrating similar changes between the aged and unaged conditions.
2. Significant increases in tip-up, after aging, are observed on bars T386, T402, B246, B378 and B445.
3. The highest tip-up (2.6%), after aging, is exhibited by bar T402 with three other bars having tip-up values in excess of 1%. No tip-up value above 1% was recorded prior to aging.
4. Thermal aging has resulted in a decrease in the absolute capacitance values for all of the aged bars. Consideration of the geometry of the stator bar confined within an artificial slot implies that the decrease in capacitance could be dependent upon swelling, or delamination, of the groundwall insulation. This finding will be correlated against the dimensional measurements of the bars, see below.
5. Comparison of Figure 4-7 with Figure 4-5 demonstrates some correlation between the tip-up values and the negative PD magnitudes. This finding is not surprising because both parameters are measures of void content in the insulation.

Generally, the results of the capacitance and dissipation factor tests indicate that at least some of the bars, especially T386, T402, B246, B378 and B445, have undergone detectable aging due to the method employed in this project. Further, evidence of correlation with the PD results shows that some further delamination of the groundwall insulation has occurred. Conversely, some of the bars, specifically T29, T42, T321 and B239, exhibit power frequency diagnostic values that are not consistent with deterioration of the insulation.

4.2 Dimensional Measurements

Dimensional measurements of the height and width of the bars were made at five equidistant points on each bar. The summary of these measurements, made prior to aging, are shown in Table 4-6. The corresponding dimensional data is contained in Table 4-7.

Table 4-6
Dimensional measurements of bars, pre-aging

Bar	Mean Height (in.)	Std. Dev'n (in.)	Mean Width (in.)	Std. Dev'n (in.)
T5	2.721	0.008	1.116	0.003
T29	2.731	0.012	1.123	0.004
T42	2.722	0.007	1.122	0.008
T218	2.731	0.006	1.121	0.005
T321	2.721	0.007	1.121	0.007
T340	2.721	0.004	1.120	0.006
T386	2.721	0.005	1.122	0.003
T402	2.722	0.002	1.110	0.003
B239	2.718	0.006	1.120	0.003
B246	2.714	0.004	1.116	0.004
B378	2.722	0.002	1.110	0.003
B445	2.716	0.004	1.121	0.002

Table 4-7
Dimensional measurements of bars, post-aging

Bar	Mean Height (in.)	Std. Dev'n (in.)	Mean Width (in.)	Std. Dev'n (in.)
T5	2.728	0.007	1.118	0.005
T29	2.762	0.019	1.139	0.008
T42	2.764	0.019	1.140	0.016
T218	2.762	0.013	1.131	0.019
T321	2.760	0.025	1.122	0.006
T340*	2.722	0.004	1.121	0.004
T386	2.768	0.021	1.151	0.022
T402	2.778	0.031	1.164	0.065
B239	2.757	0.023	1.133	0.015
B246	2.757	0.024	1.138	0.011
B378	2.764	0.030	1.139	0.006
B445	2.758	0.027	1.142	0.014

* this bar not aged because of failure during high voltage diagnostic tests on initial cycle.

4.3 Dielectric Spectroscopy Test Results

Low frequency dielectric spectroscopy, hereafter referred to as DS, measurements on the stator bars prior to, and after, thermal aging, were performed using commercially available equipment. Initial measurements before aging were accomplished using a WaBTech AB Insulation Diagnosis Analyzer. During the course of the project, this instrument was upgraded and post-aging DS results were obtained using a IDA 200 instrument equipped with a high voltage interface unit. This device is a so-called active bridge, i.e., there is no reference capacitor. Instead, the reference signal is derived by generating a signal in phase quadrature to that measured on the test object. The dielectric loss is related to the phase difference between the two signals. The test voltage of up to 20 kV rms is obtained using an amplifier (Trek 20/20). Both bridge and power supply are under computer control and the entire measurement sequence is automated. Typically, measurements are made at several voltages across three decades of frequency. Similar to the capacitance and dissipation factor measurements described previously, the DS data was obtained with the samples unguarded.

4.3.1 Dielectric Spectroscopy Results – Prior to Aging

The results of DS testing for the stator bars prior to undergoing thermal aging are illustrated in Figures 4-10 through 4-20 in which $\tan\delta$ (dissipation factor) is plotted as a function of frequency. Initial inspection of these data show a number of common features.

1. The dielectric loss tends to increase as frequency decreases.
2. Losses increase as the applied voltage is increased. Note that at above 21 Hz, there are no data points for the higher voltages because of limitations in the high voltage amplifier used.
3. Similar to the power frequency diagnostic test results, differences between the low frequency behaviour of the stator bars also exist.

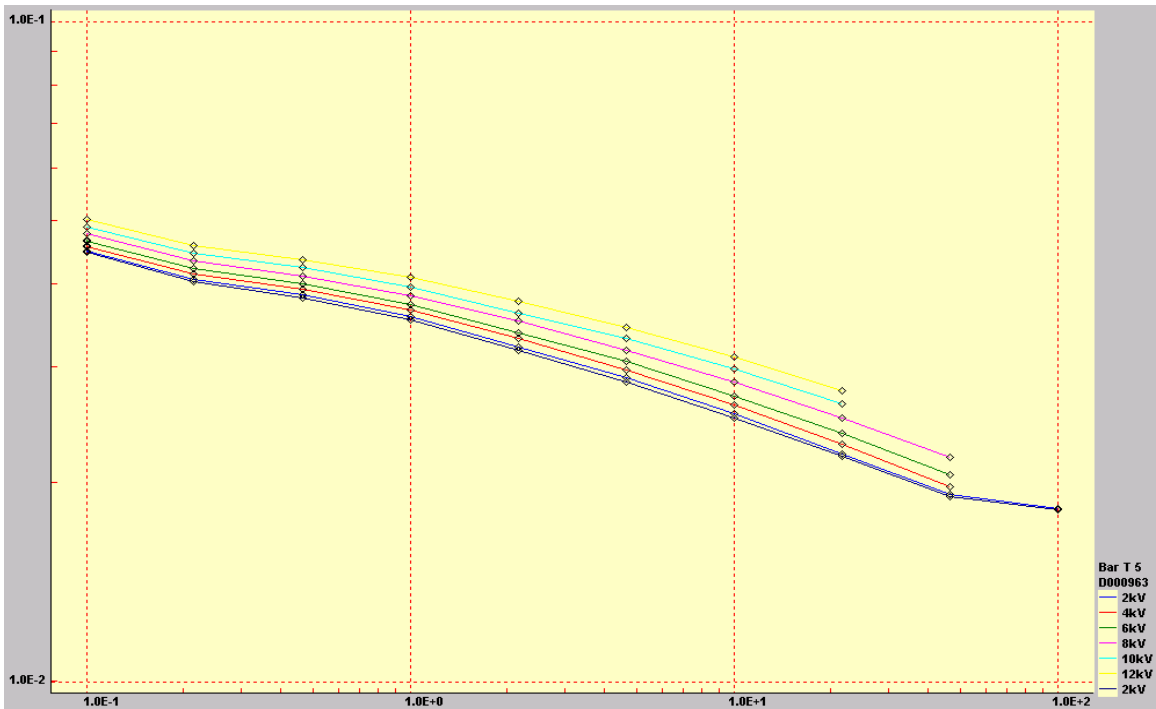


Figure 4-10
Dielectric response of bar T5, control bar

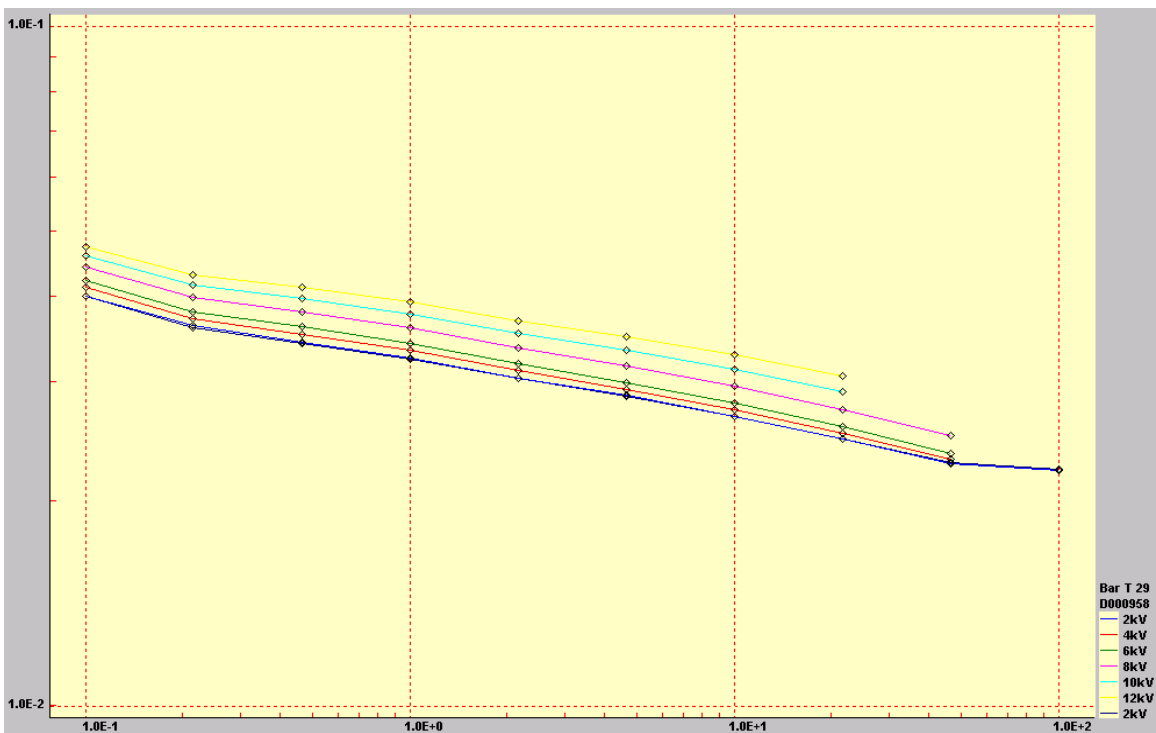


Figure 4-11
Dielectric response of bar T29, pre-aging

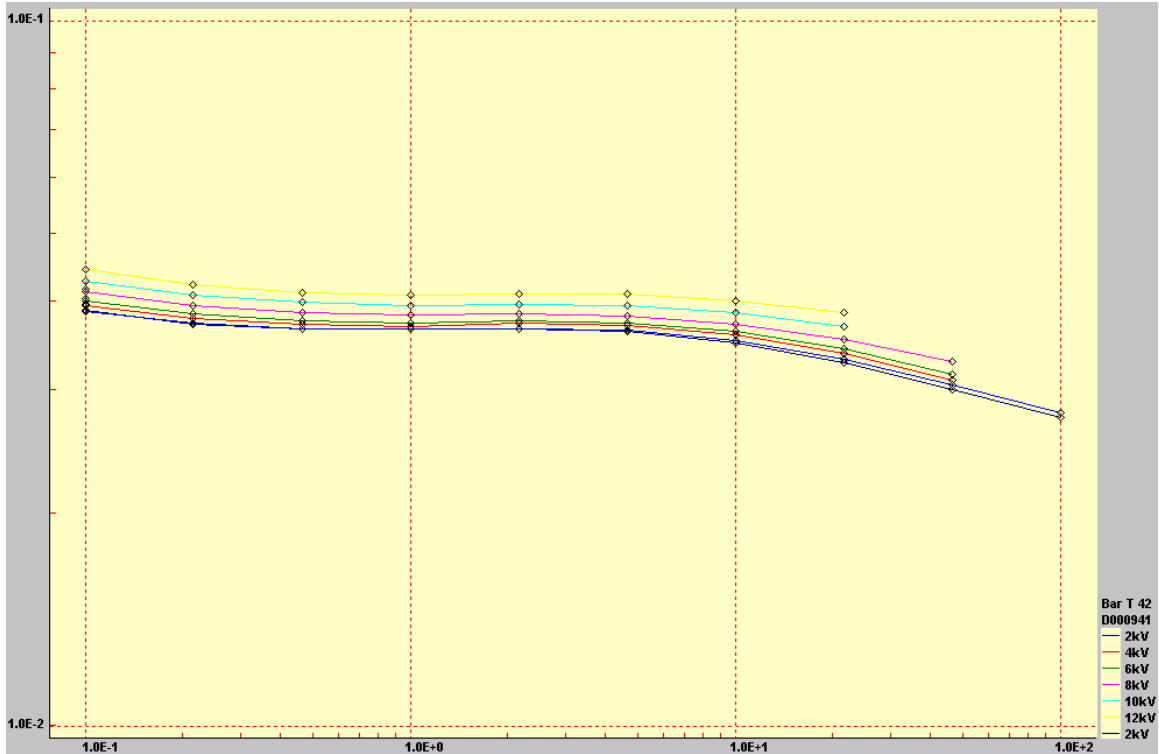


Figure 4-12
Dielectric response of bar T42, pre-aging

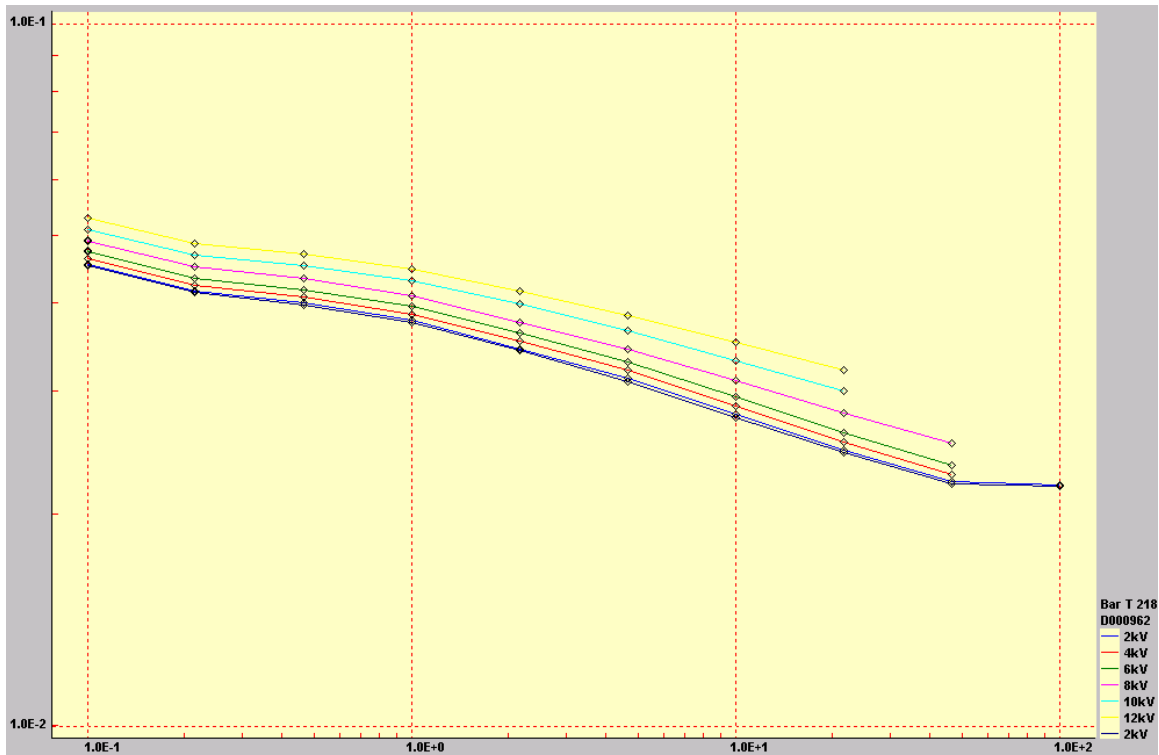


Figure 4-13
Dielectric response of bar T218, pre-aging

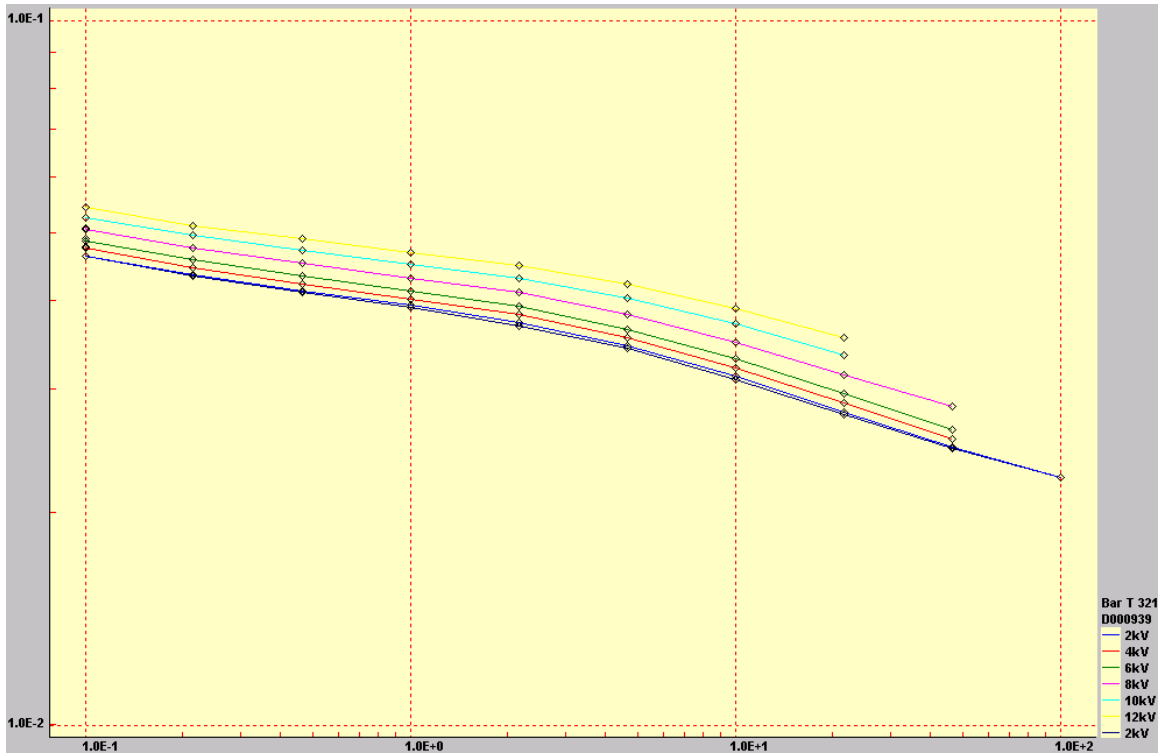


Figure 4-14
Dielectric response of bar T321, pre-aging

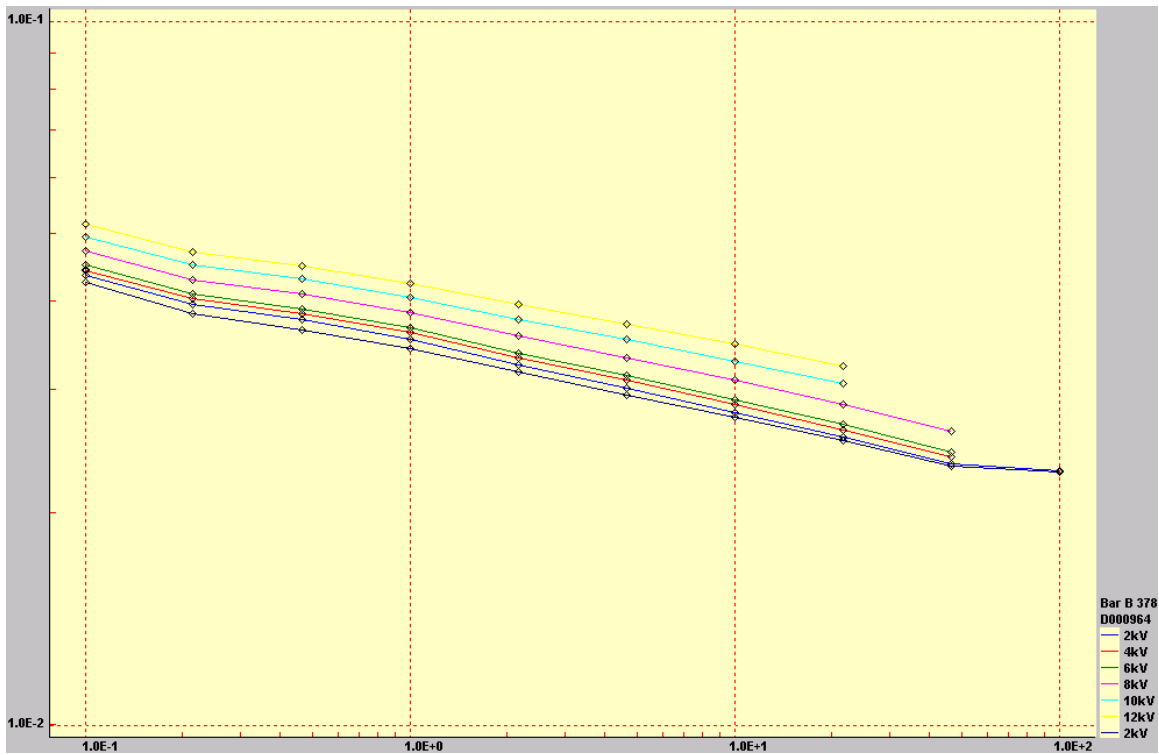


Figure 4-15
Dielectric response of bar B378, pre-aging

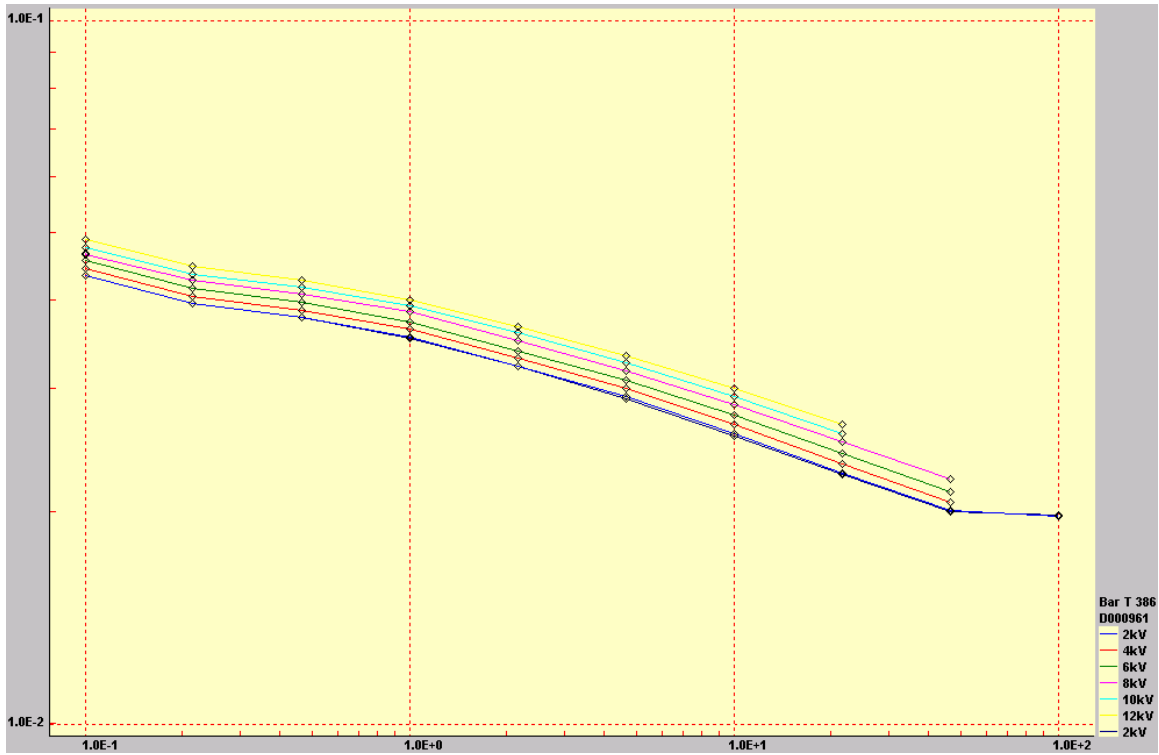


Figure 4-16
Dielectric response of bar T386, pre-aging

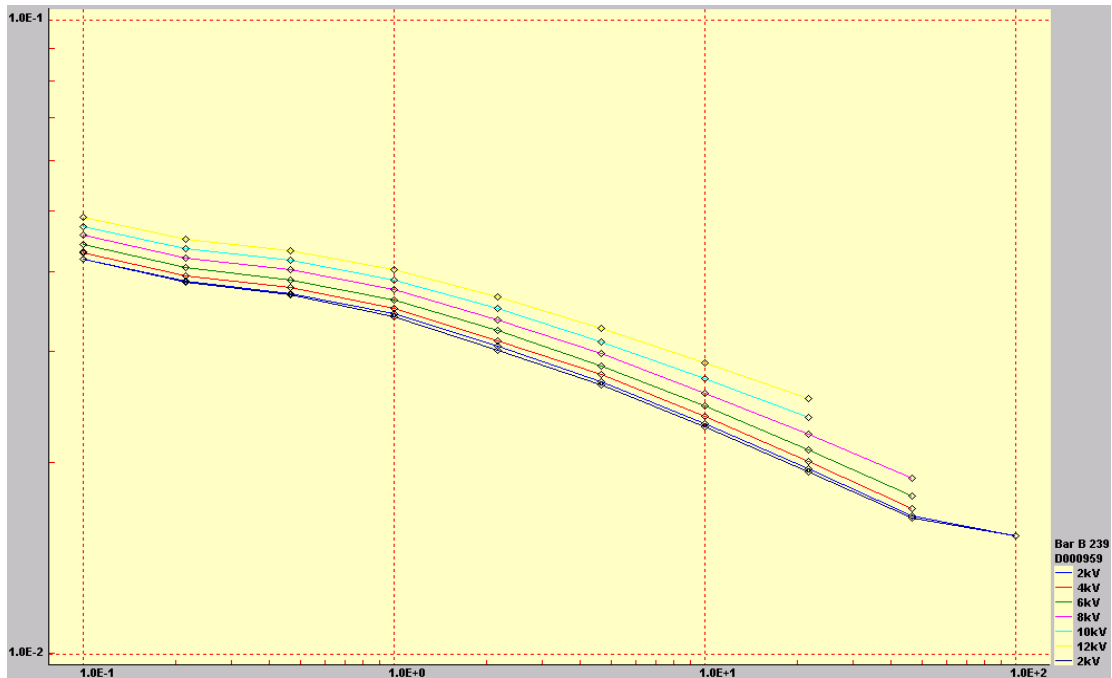


Figure 4-17
Dielectric response of bar B239, pre-aging

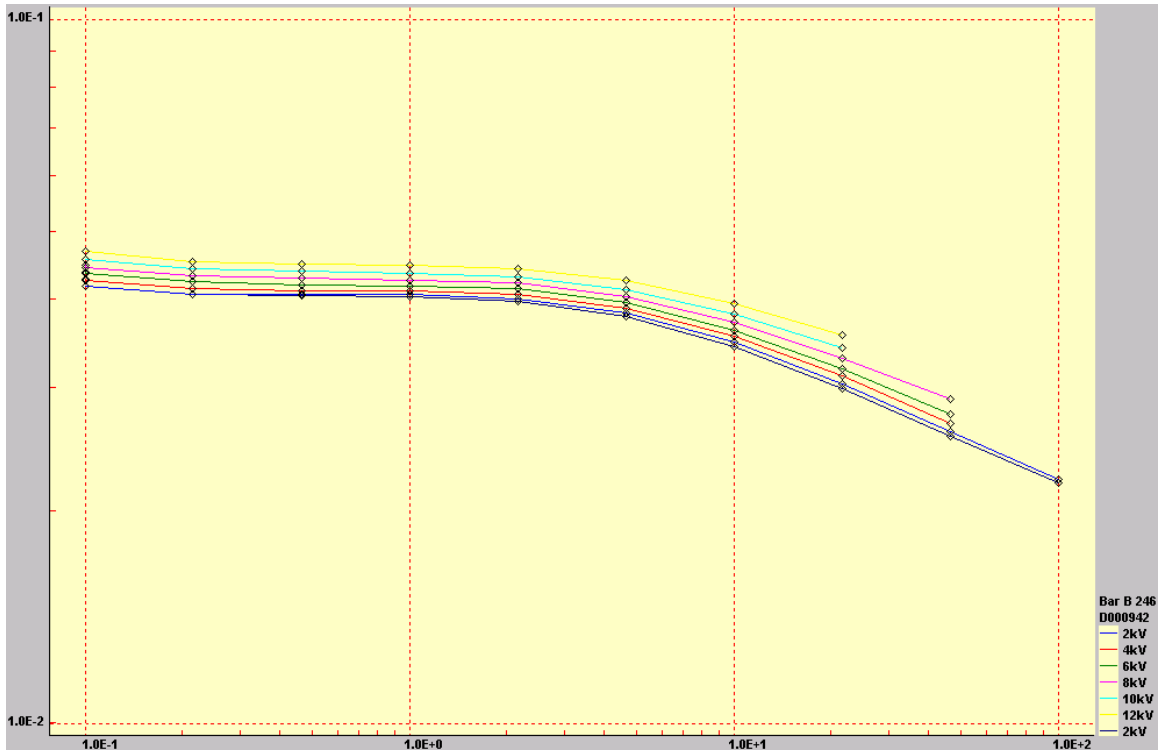


Figure 4-18
Dielectric response of bar B246, pre-aging

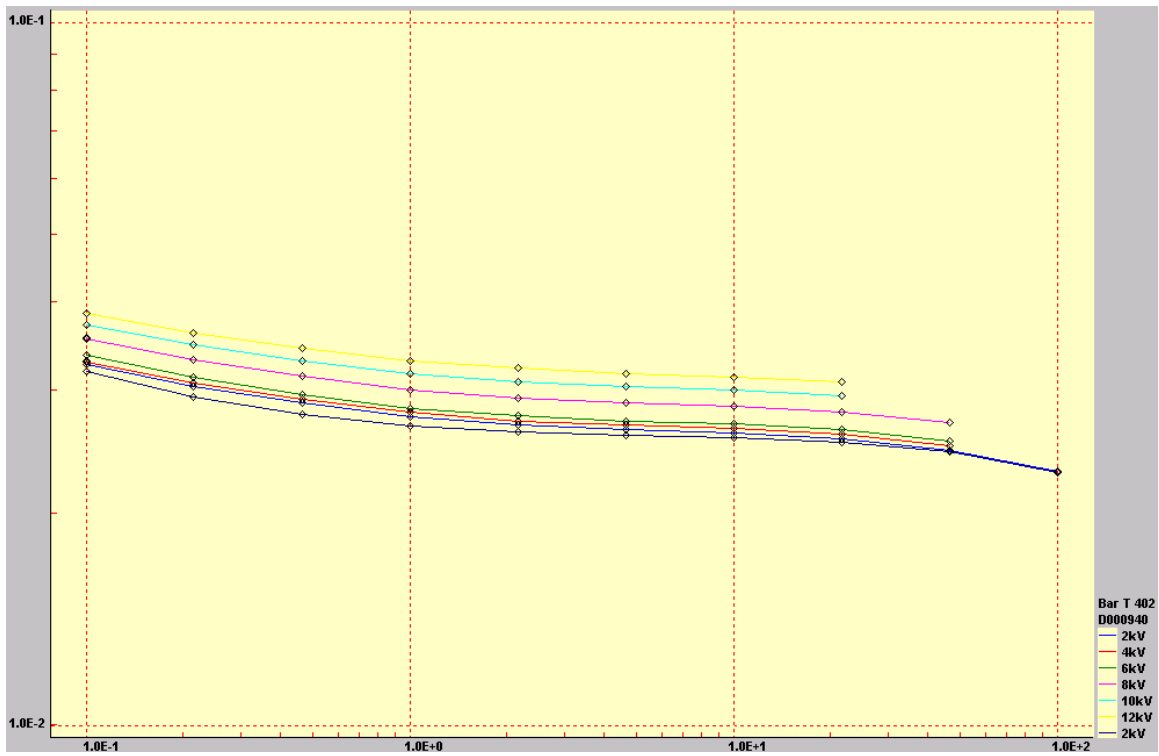


Figure 4-19
Dielectric response of bar T402, pre-aging

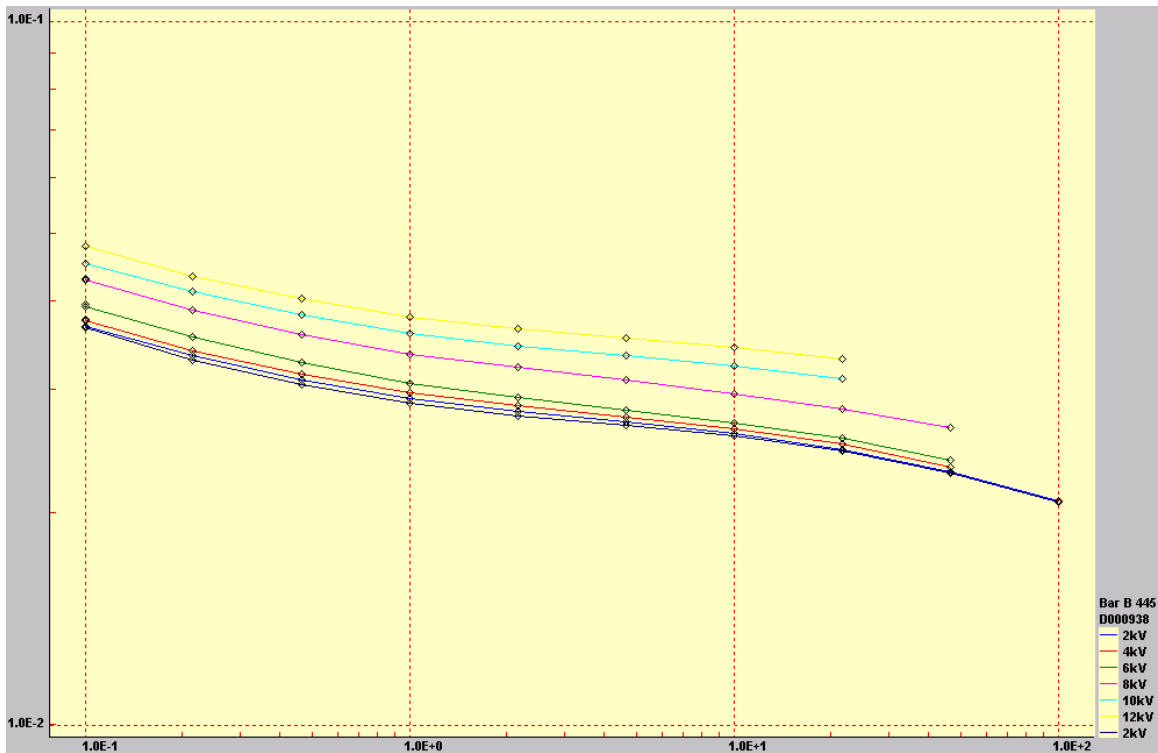


Figure 4-20
Dielectric response of bar B445, pre-aging

4.3.2 Dielectric Spectroscopy Results – After Aging

The results of DS testing for the stator bars subsequent to undergoing thermal aging are illustrated in Figures 4-21 through 4-31 in which $\tan\delta$ (dissipation factor) is plotted as a function of frequency. Table 4-8 provides a comparison between the pre- and post-aging data at 0.1 and 10 Hz (the highest frequency at which 12 kV measurements can be obtained). Table 4-9 illustrates the corresponding tip-up values.

Table 4-8
Comparison of $\tan \delta$ of aged and unaged bars at two frequencies

Bar	Dissipation Factor ($\tan\delta$)							
	Pre-Aging				Post-Aging			
	10 Hz		0.1 Hz		10 Hz		0.1 Hz	
	2 kV	12 kV	2 kV	12 kV	2 kV	12 kV	2 kV	12 kV
T5	2.54	3.11	4.49	5.0	2.08	2.59	4.75	5.25
T29	2.67	3.28	4.01	4.73	3.01	3.52	4.72	5.51
T42	3.52	4.01	3.88	4.43	2.66	3.39	4.62	5.70
T218	2.78	3.52	4.54	5.29	2.20	3.28	4.71	6.14
T321	3.12	3.90	4.64	5.42	2.54	3.61	4.66	6.11
B378	2.78	3.47	4.35	5.14	3.18	5.29	4.98	7.31
T386	2.58	2.99	4.33	4.89	2.28	4.35	4.72	7.37
B239	2.31	2.88	4.20	4.87	2.08	3.28	4.31	6.06
B246	3.48	3.94	4.17	4.67	2.36	4.52	4.66	7.28
T402	2.60	3.13	3.26	3.71	2.43	5.86	3.58	6.78
B445	2.59	3.44	3.68	4.78	2.52	5.19	3.97	6.75

Table 4-9
Comparison of tip-up of aged and unaged bars at two frequencies

Bar	Pre-Aging		Post-Aging	
	Tip-Up (%) 10 Hz	Tip-Up(%) 0.1 Hz	Tip-Up (%) 10 Hz	Tip-Up (%) 0.1 Hz
T5	0.57	0.51	0.51	0.50
T29	0.61	0.72	0.41	0.79
T42	0.49	0.55	0.73	1.08
T218	0.74	0.75	1.08	1.43
T321	0.78	0.78	1.07	1.45
B378	0.69	0.79	2.11	2.33
T386	0.41	0.56	2.07	2.65
B239	0.57	0.67	1.20	1.75
B246	0.46	0.50	2.16	2.62
T402	0.53	0.45	3.43	3.20
B445	0.85	1.10	2.67	2.78

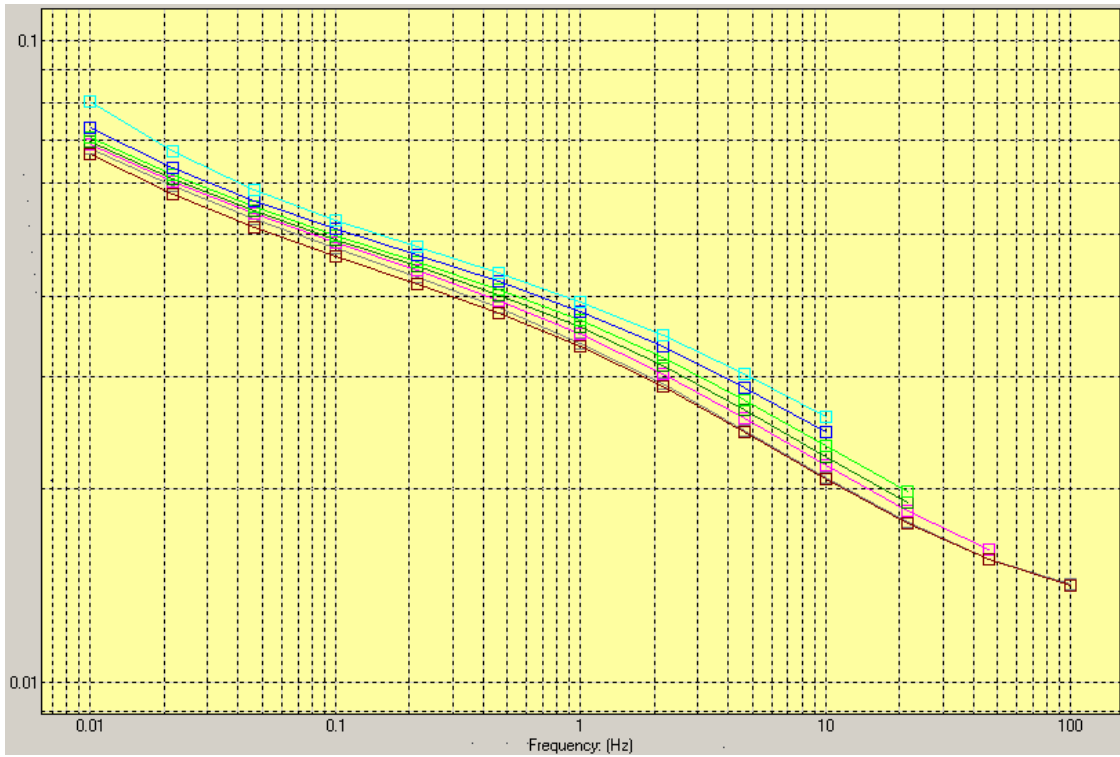


Figure 4-21
Dielectric response of bar T5, control bar

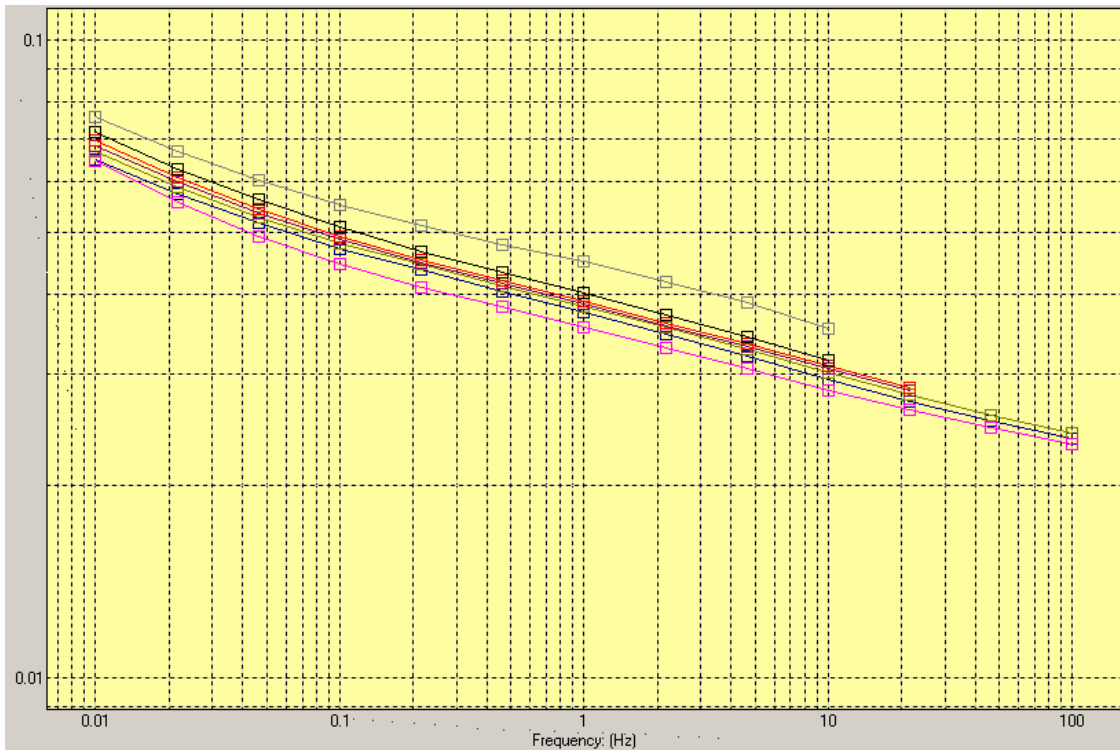


Figure 4-22
Dielectric response of bar T29, post-aging

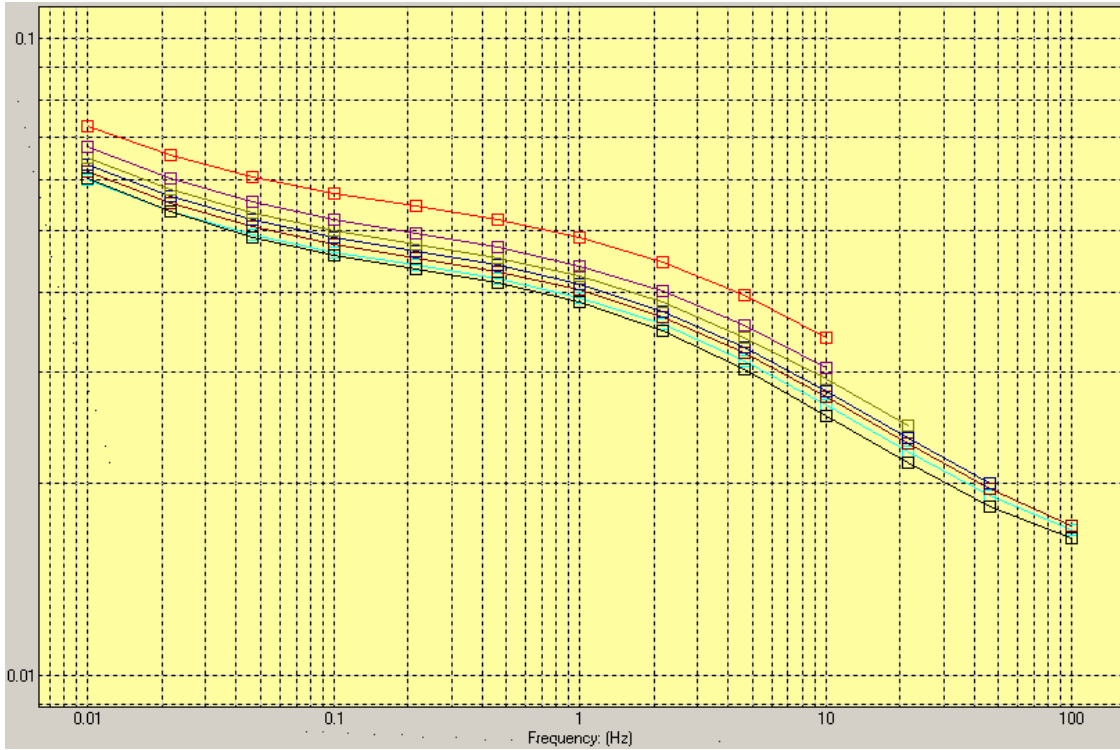


Figure 4-23
Dielectric response of bar T42, post-aging

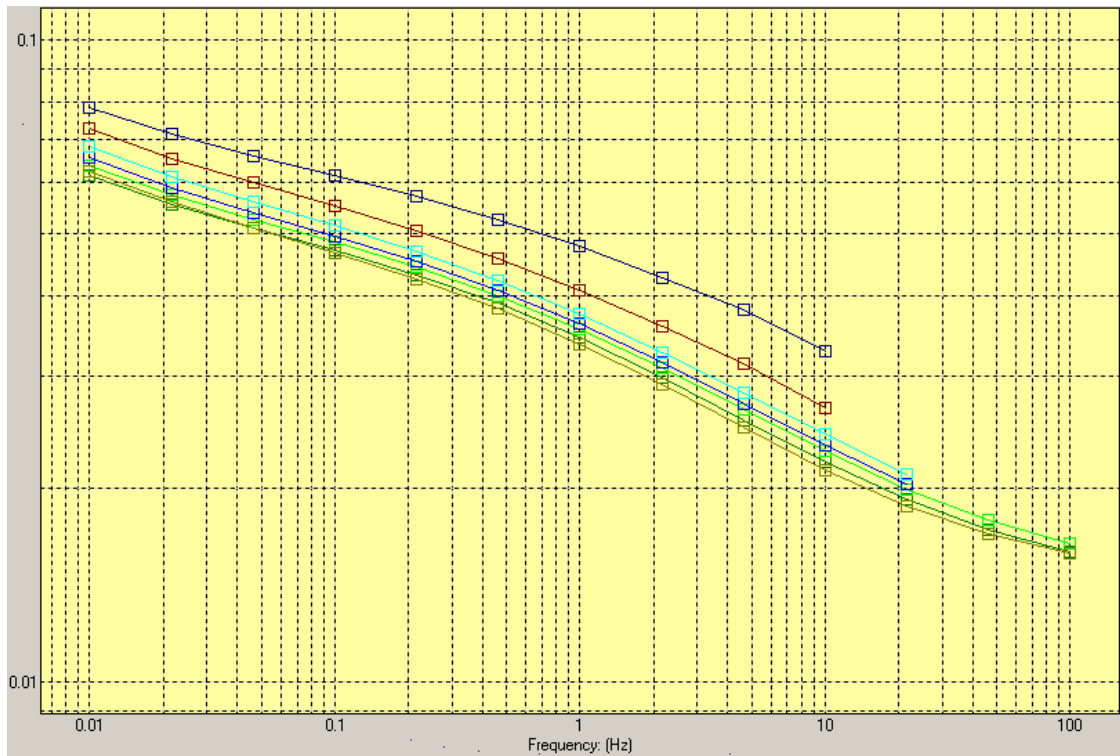


Figure 4-24
Dielectric response of bar T218, post-aging

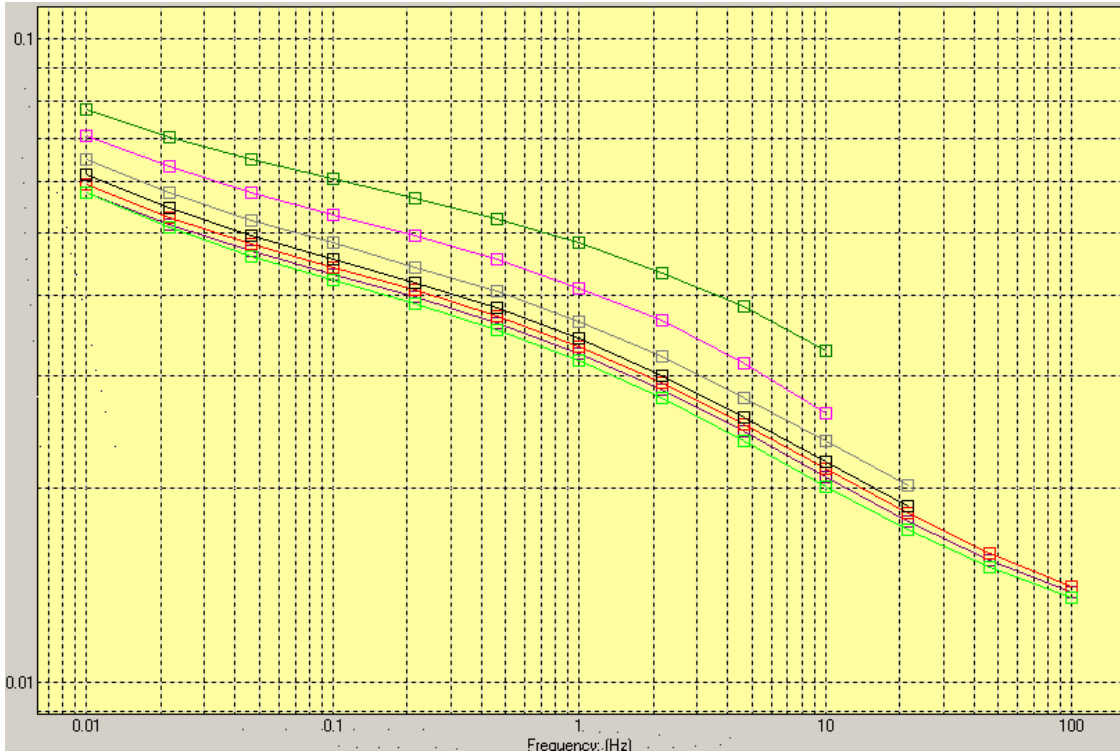


Figure 4-25
Dielectric response of bar B239, post-aging

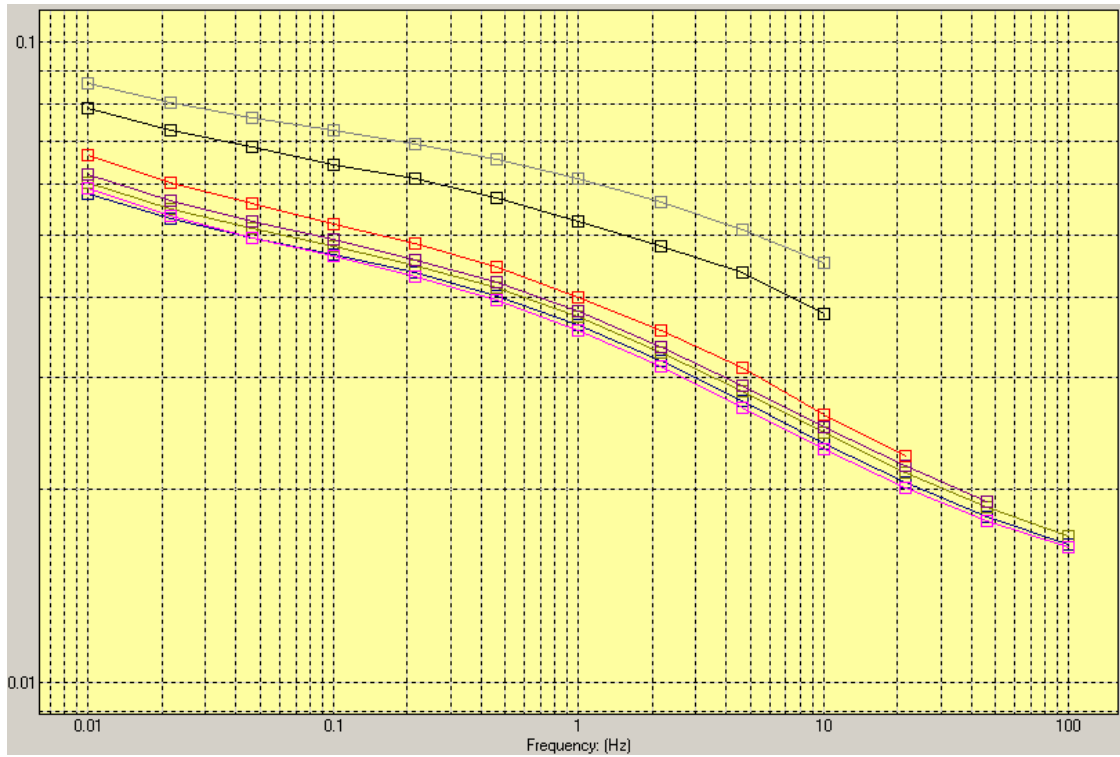


Figure 4-26
Dielectric response of bar B246, post-aging

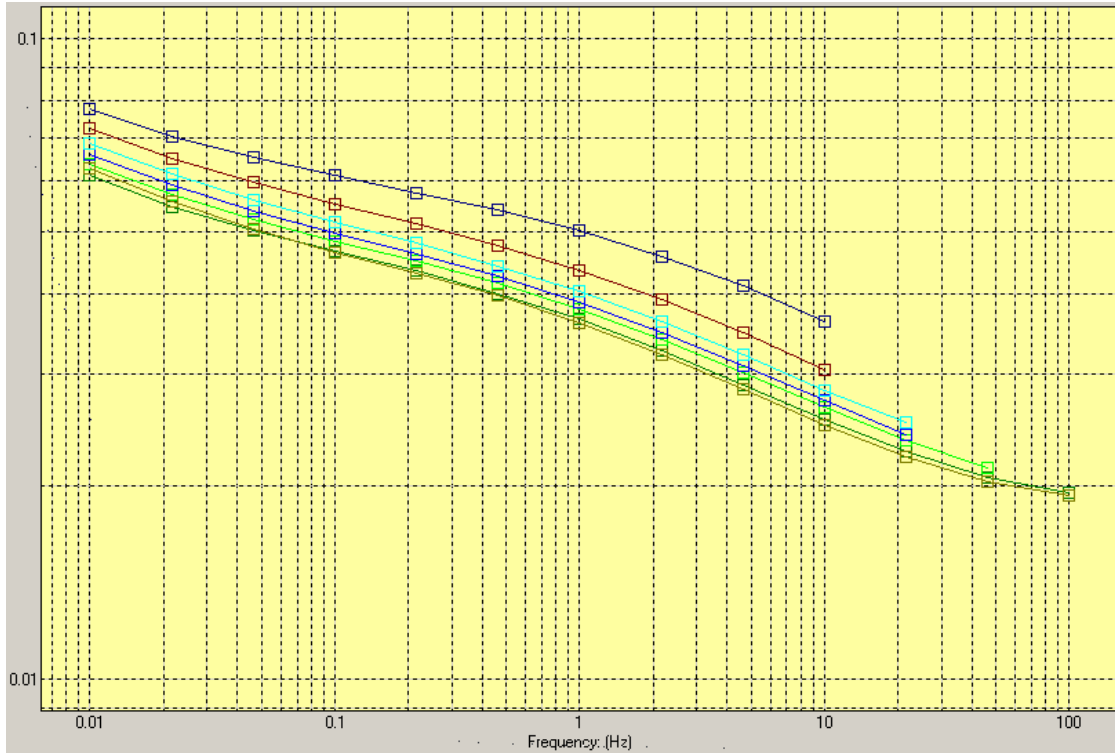


Figure 4-27
Dielectric response of bar B321, post-aging

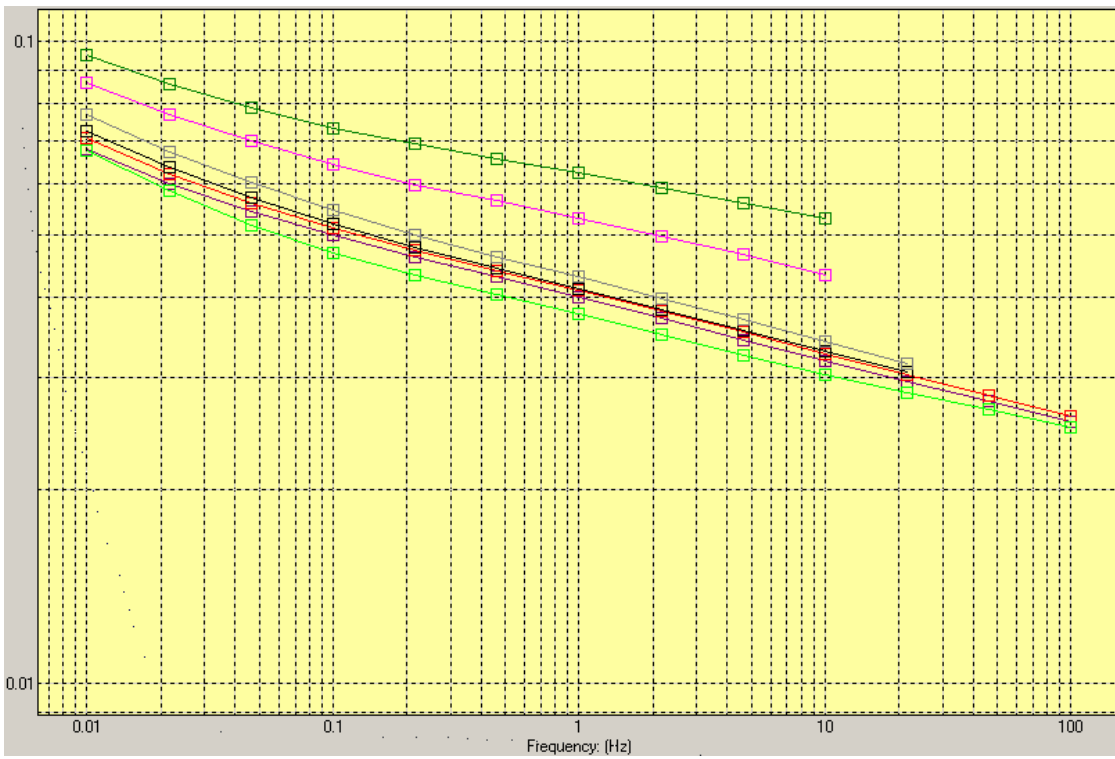


Figure 4-28
Dielectric response of bar B378, post-aging

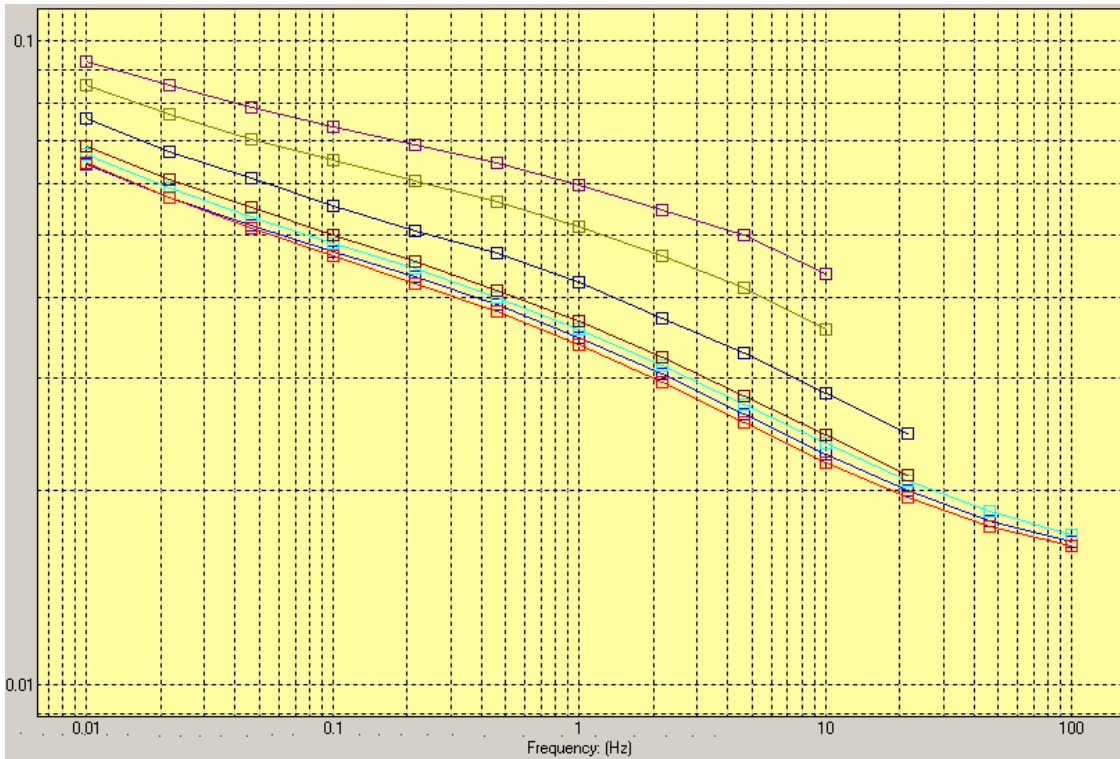


Figure 4-29
Dielectric response of bar T386, post-aging

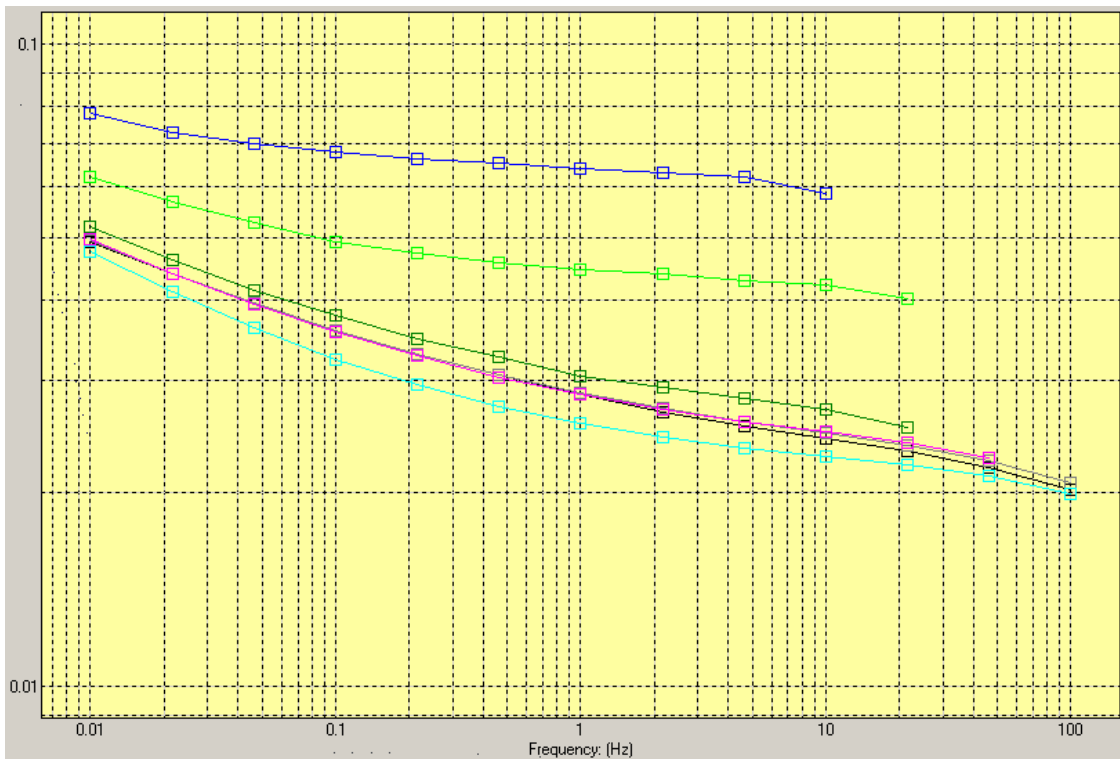


Figure 4-30
Dielectric response of bar T402, post-aging

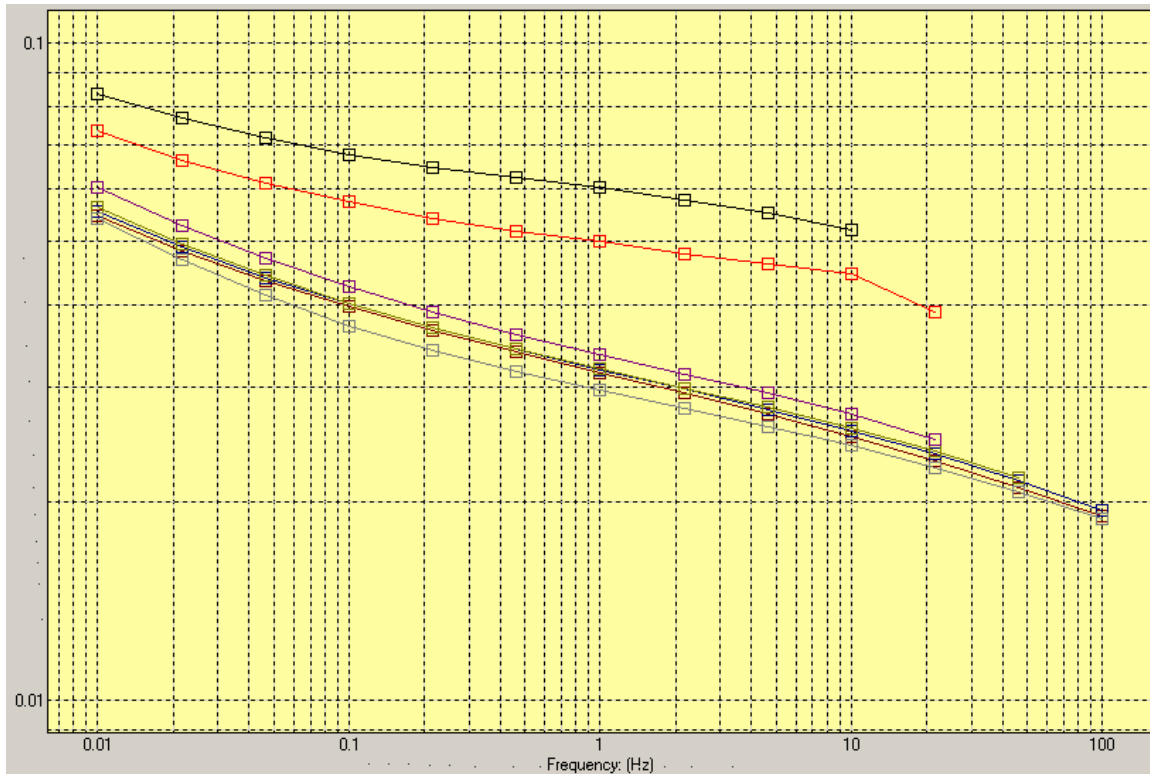


Figure 4-31
Dielectric response of bar B445, post-aging

4.4 Return Voltage Measurement Results

The RVM test results are presented in Figures 4-32 through 4-53. Two key parameters of the test are the maximum return voltage (V_{\max}) and the time to achieve this value (T_c). These data, for unaged and aged conditions, are recorded in Table 4-10 and were obtained by charging the bar for 60 s with 1 kV dc, discharging for 15 s then measuring for a period sufficient to record the maximum return voltage.

Table 4-10
Comparison of RVM results before and after aging

Bar	V _{max} (V) pre-age	T _c (s) pre-age	V _{max} (V) post-age	T _c (s) post-age
T5	47.0	430	51.6	458
T29	48.9	701	52.4	459
T42	49.6	671	45.2	518
T218	59.5	661	45.0	543
T321	53.1	501	45.3	482
B378	47.3	612	54.5	1027
T386	50.5	661	45.6	491
B239	48.4	567	44.7	544
B246	49.0	617	43.4	557
T402	38.0	622	36.8	592
B445	47.9	581	43.0	554

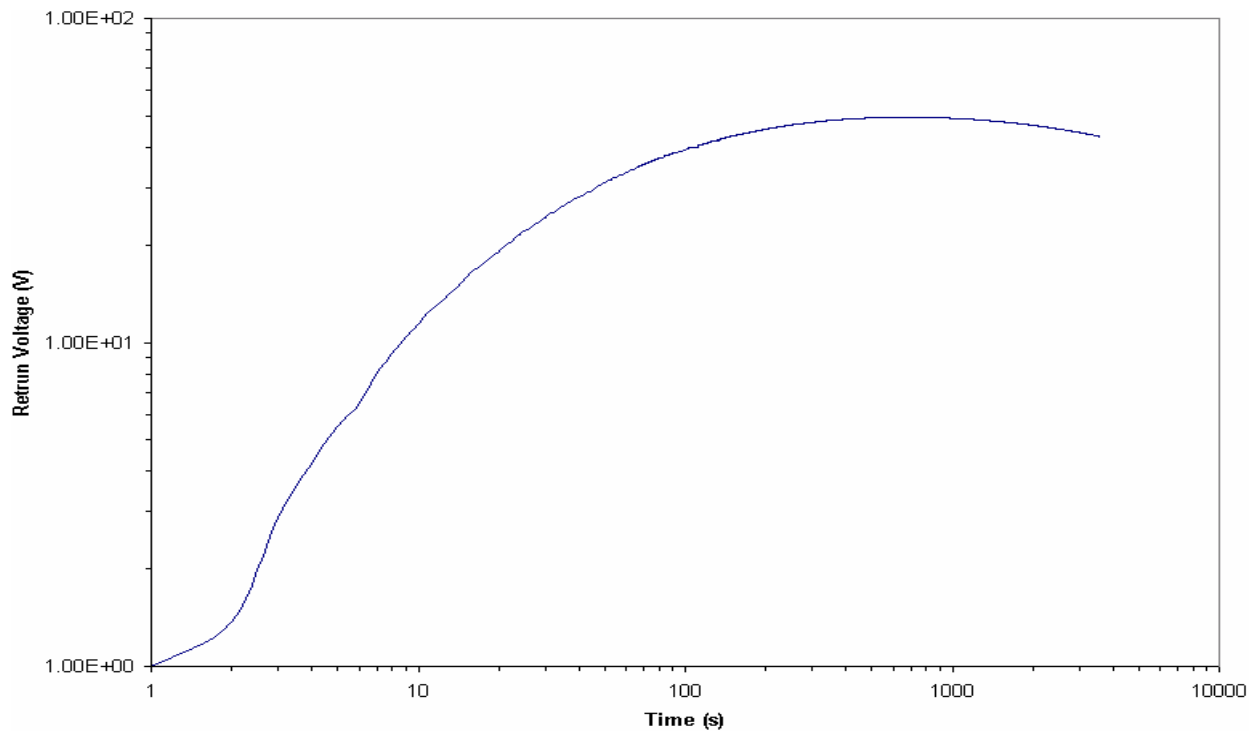


Figure 4-32
RVM response of bar T5, control bar

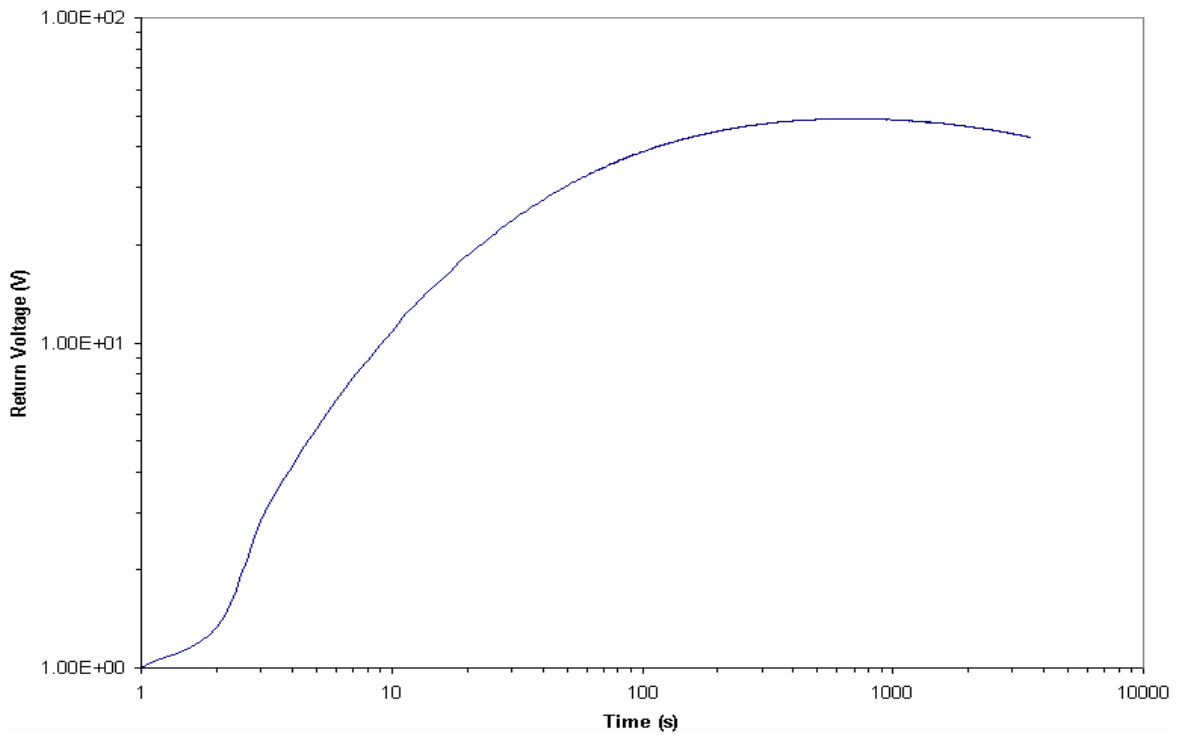


Figure 4-33
RVM response of bar T29, pre-aging

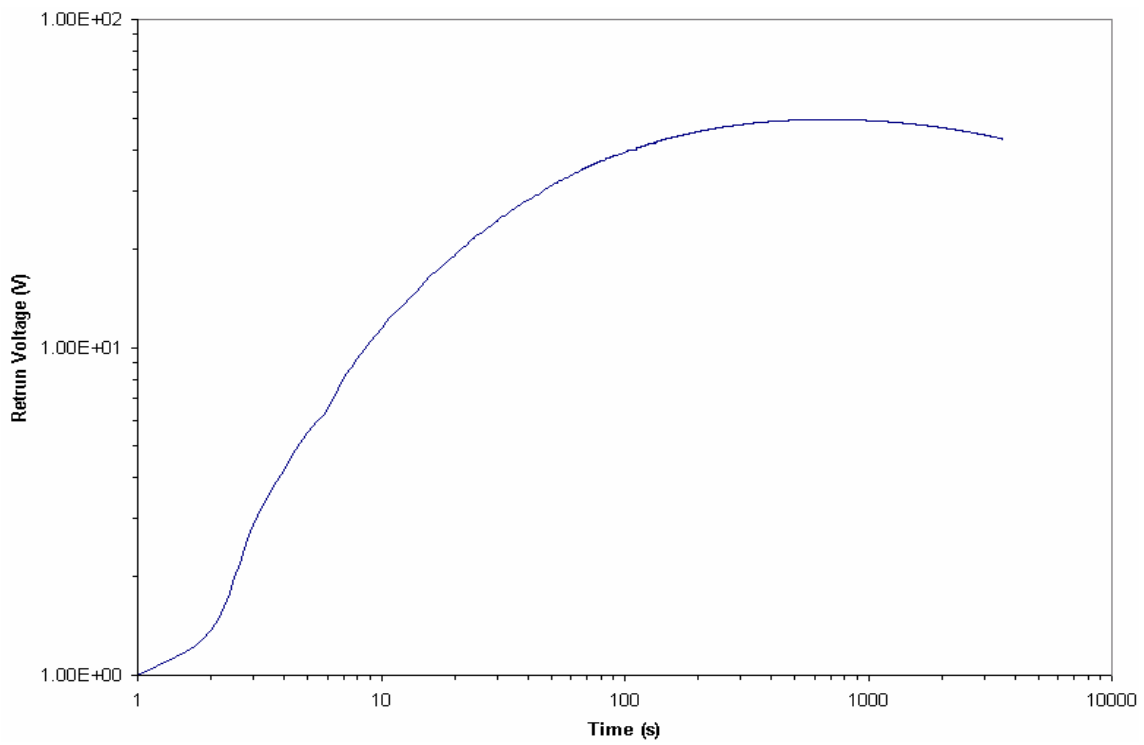


Figure 4-34
RVM response of bar T42, pre-aging

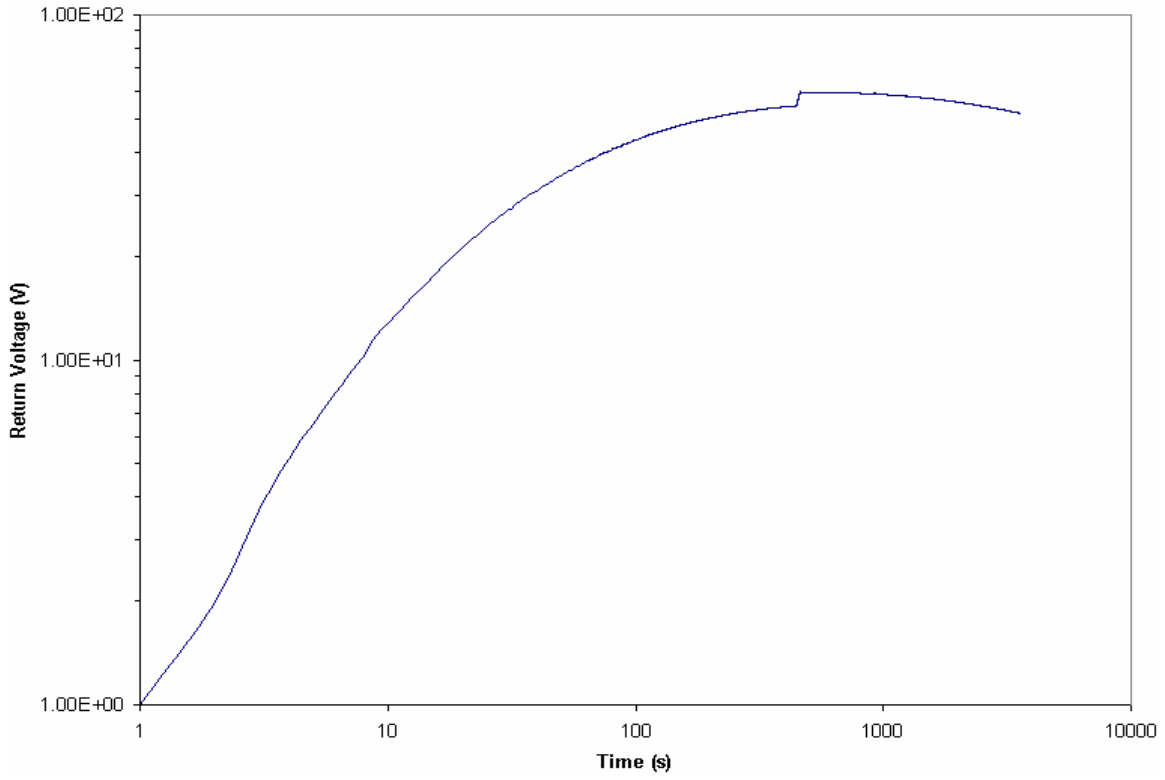


Figure 4-35
RVM response of bar T218, pre-aging

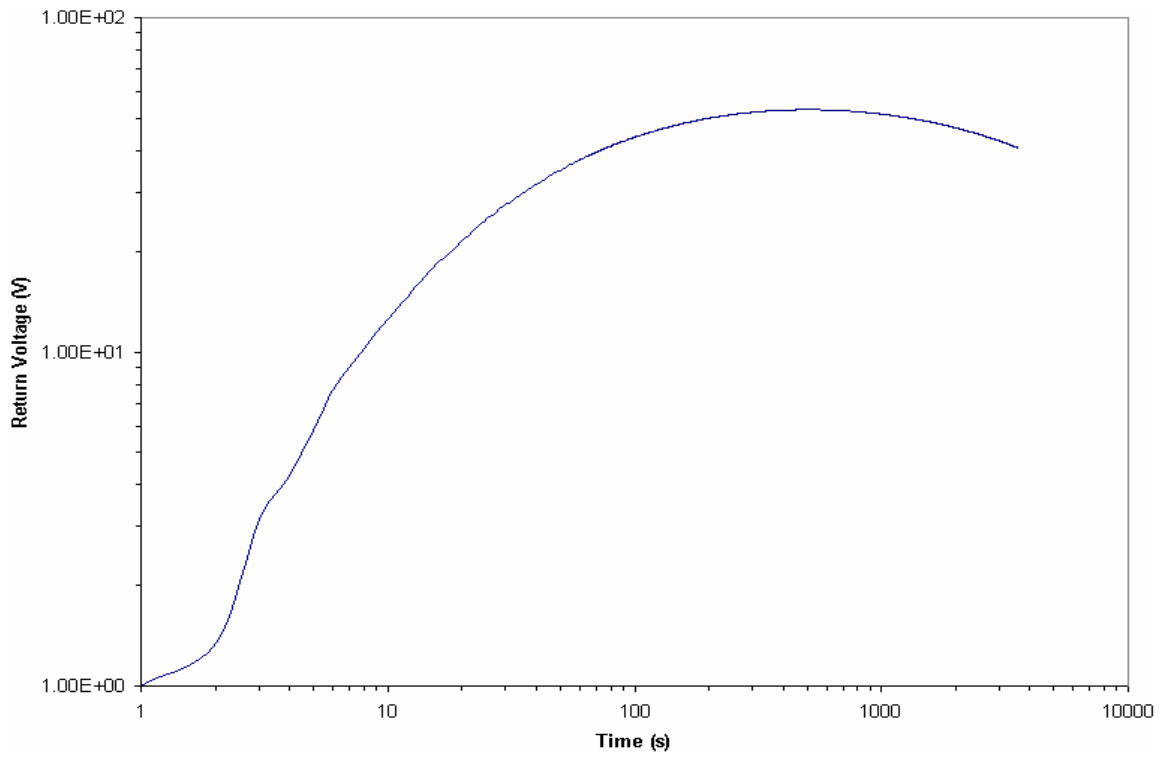


Figure 4-36
RVM response of bar T321, pre-aging

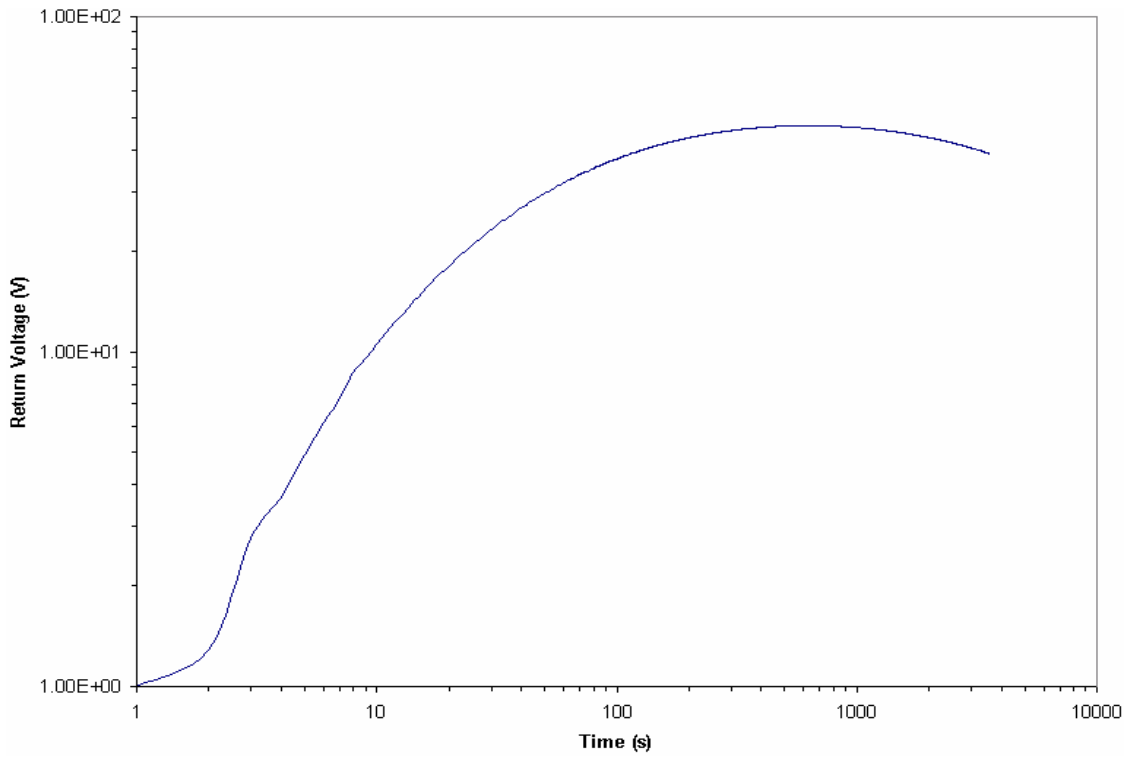


Figure 4-37
RVM response of bar B378, pre-aging

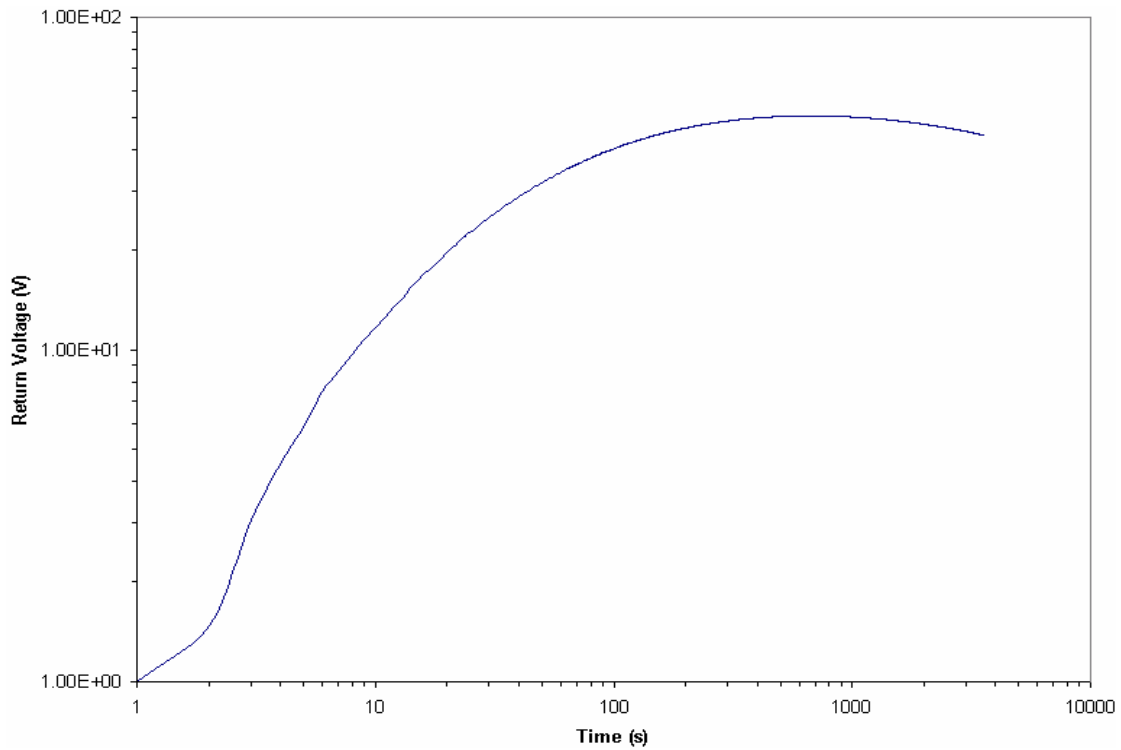


Figure 4-38
RVM response of bar T386, pre-aging

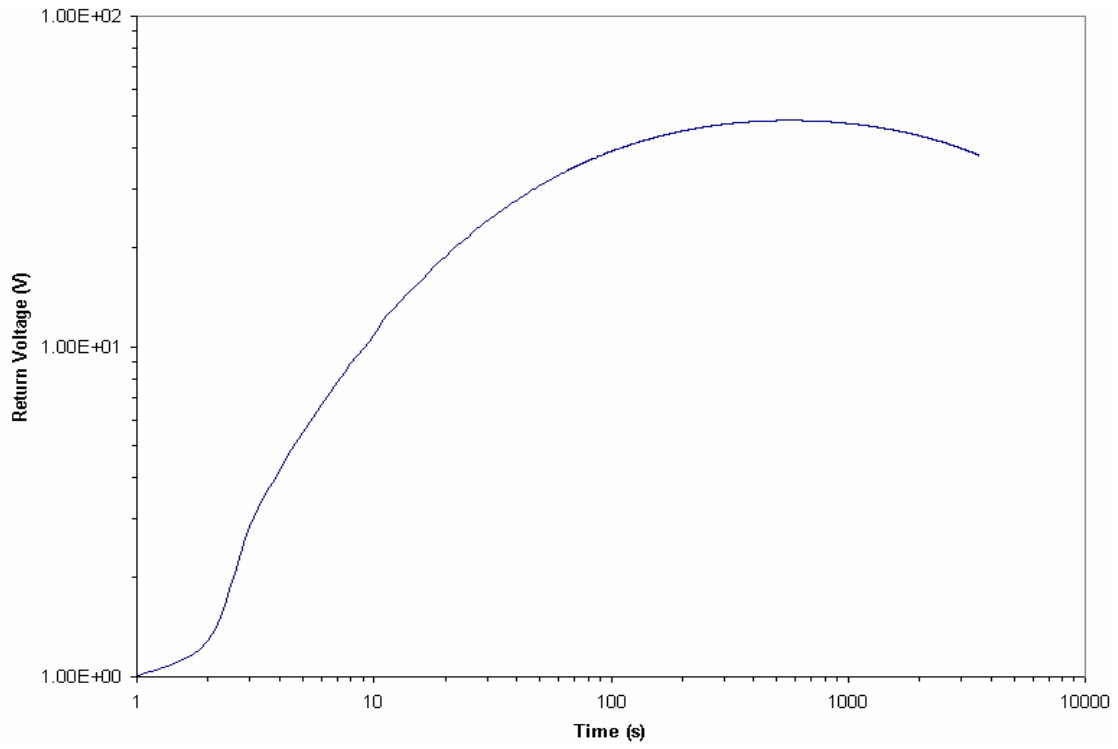


Figure 4-39
RVM response of bar B239, pre-aging

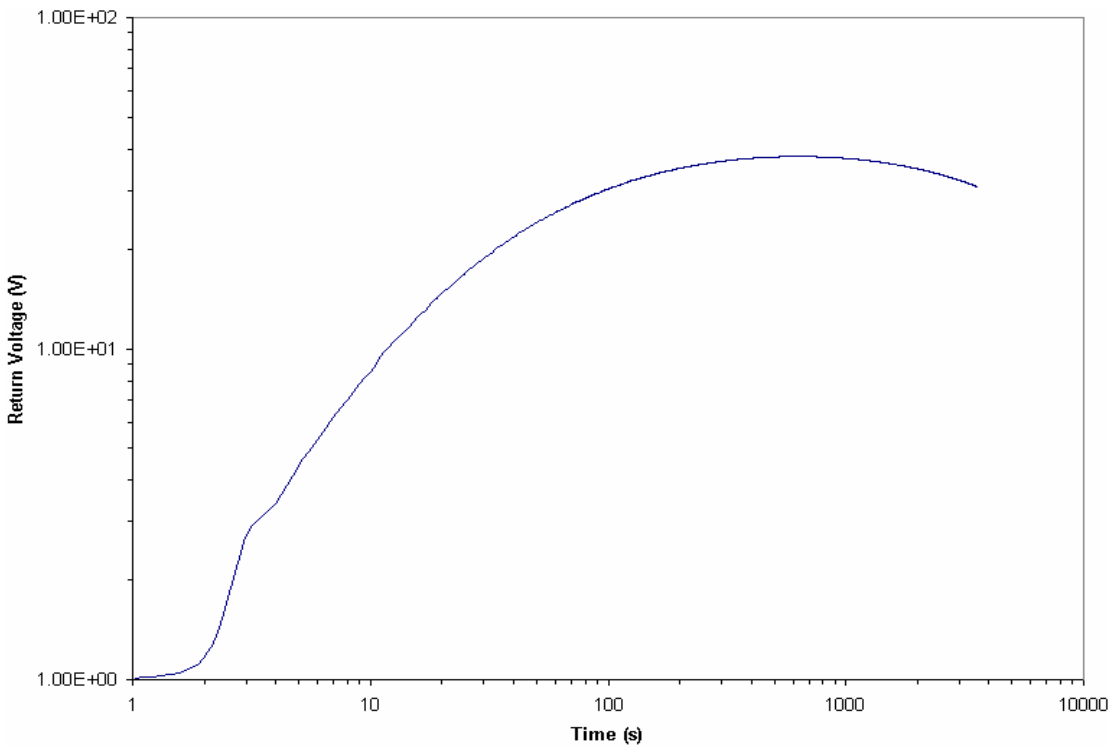


Figure 4-40
RVM response of bar B246, pre-aging

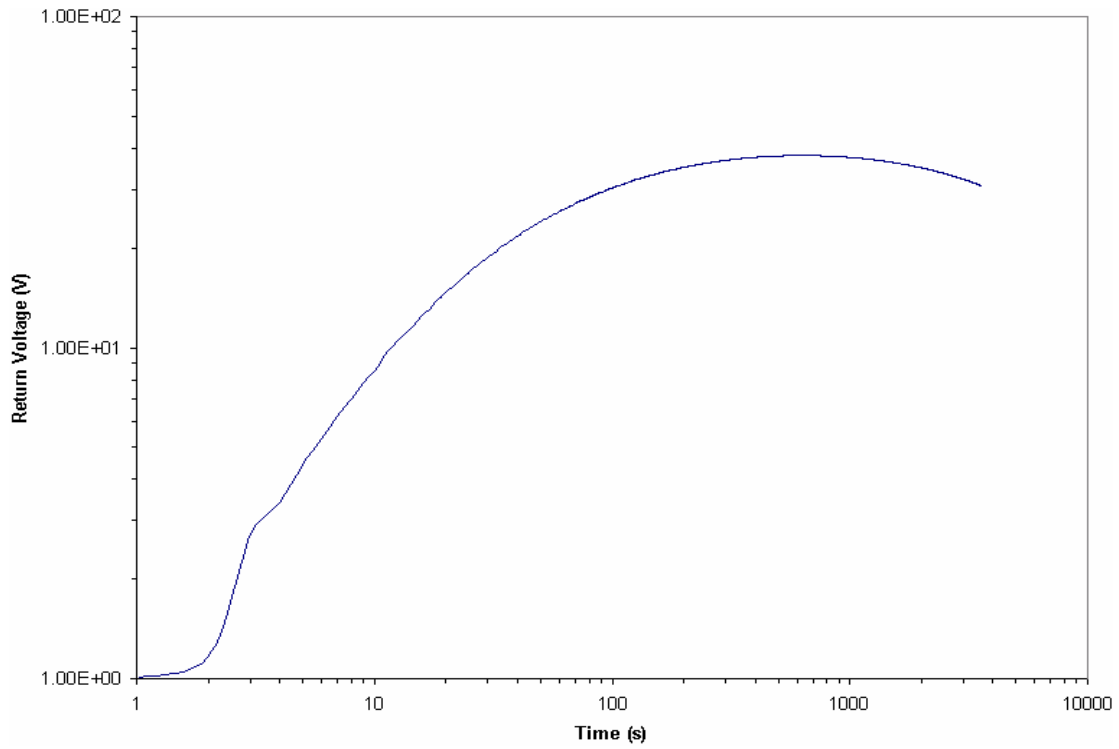


Figure 4-41
RVM response of bar T402, pre-aging

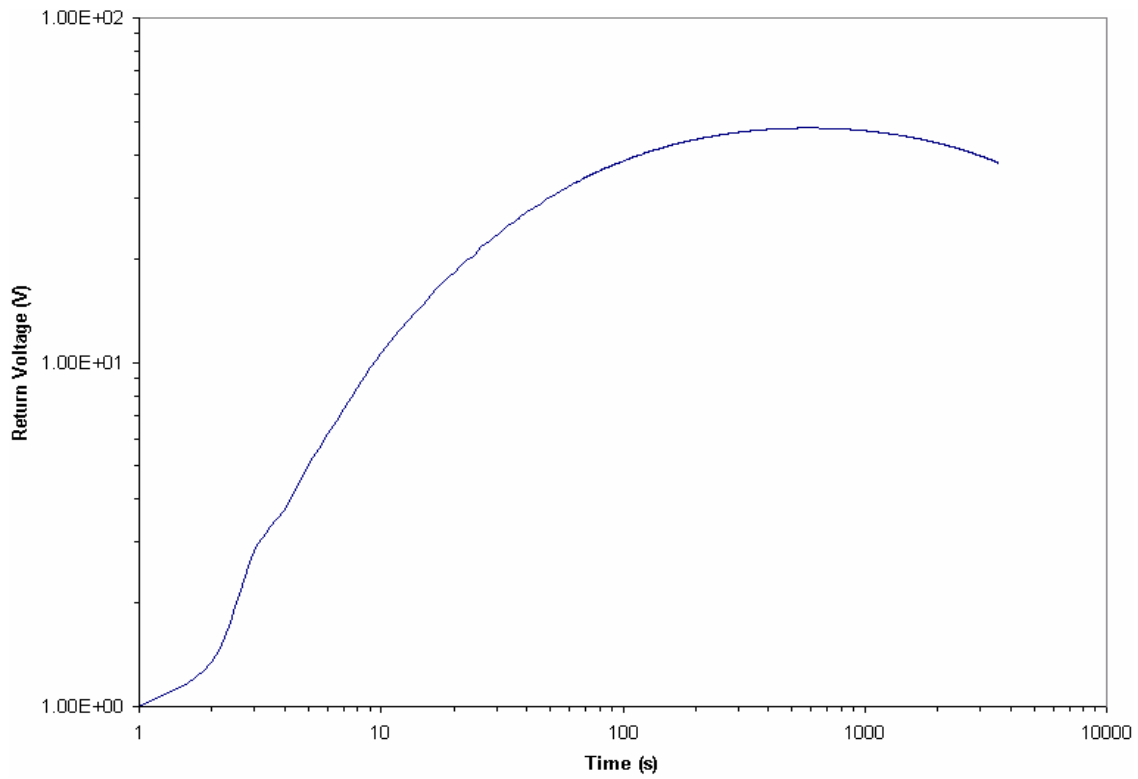


Figure 4-42
RVM response of bar B445, pre-aging

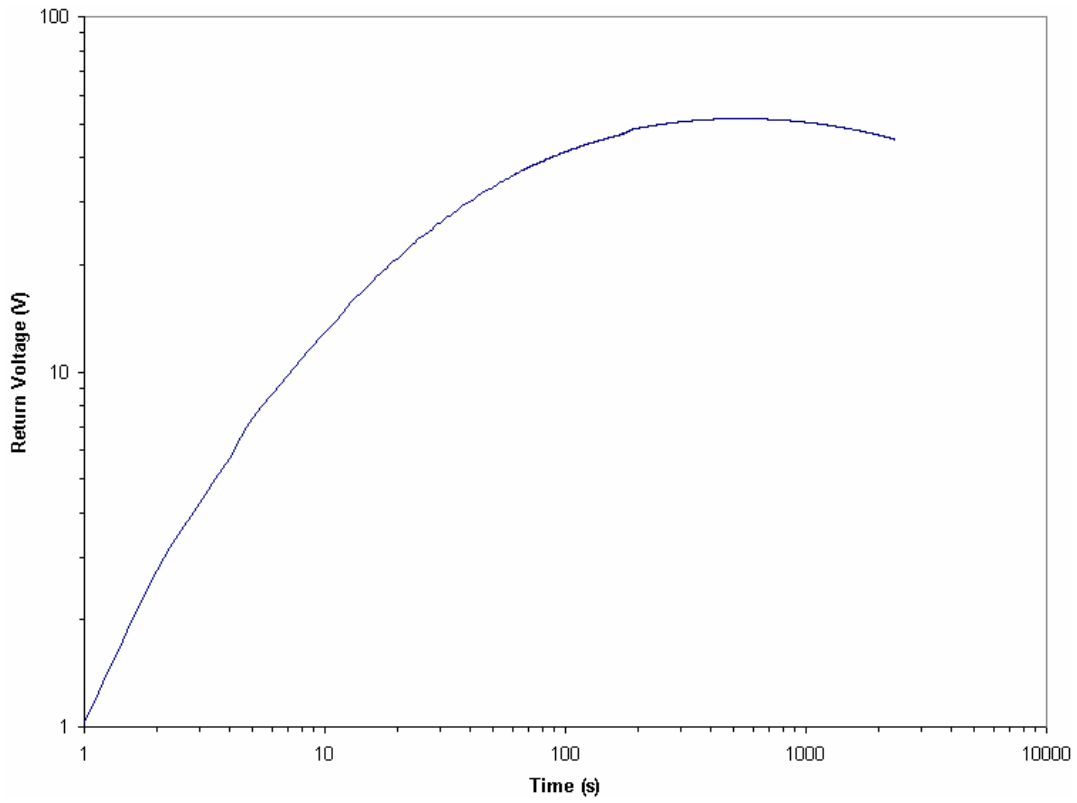


Figure 4-43
RVM response of bar T5, control bar

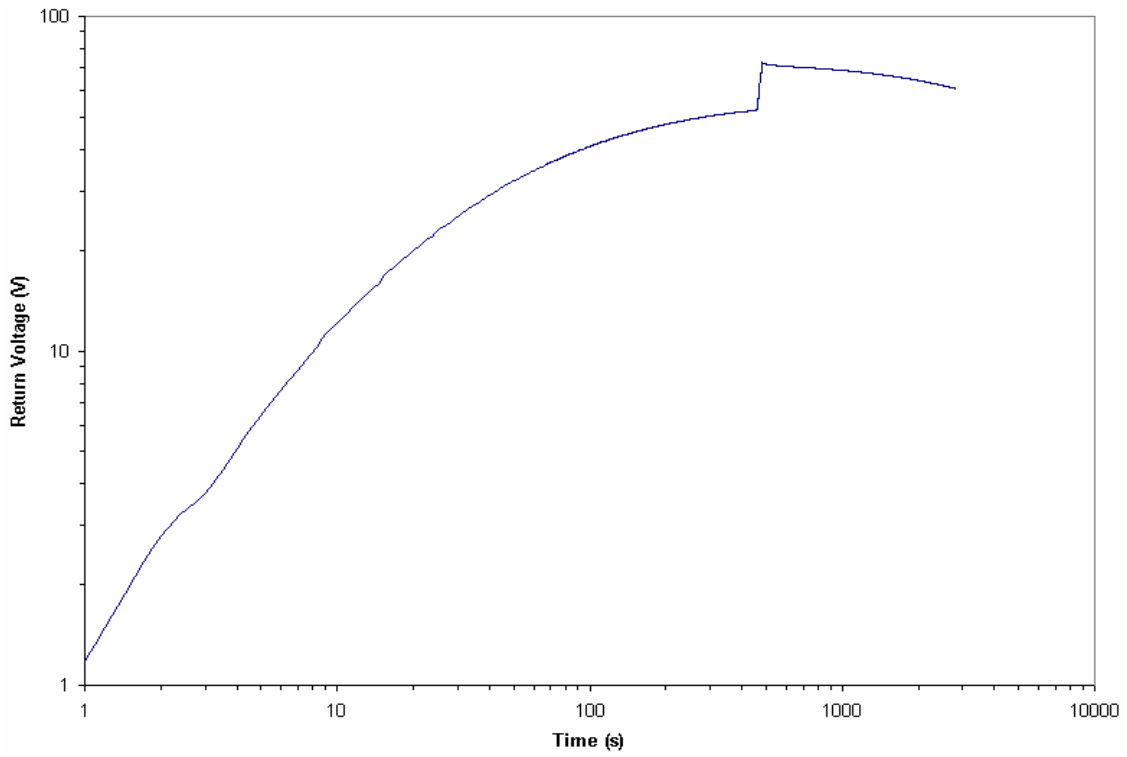


Figure 4-44
RVM response of bar T29, post-aging

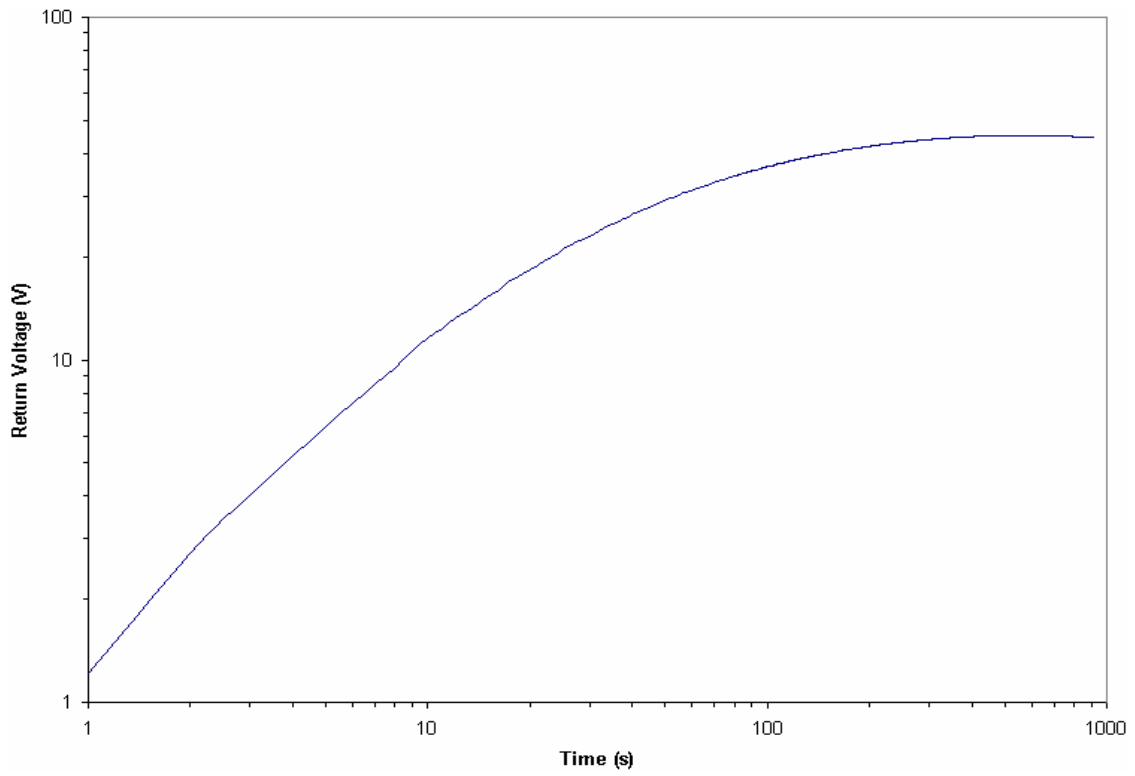


Figure 4-45
RVM response of bar T42, post-aging

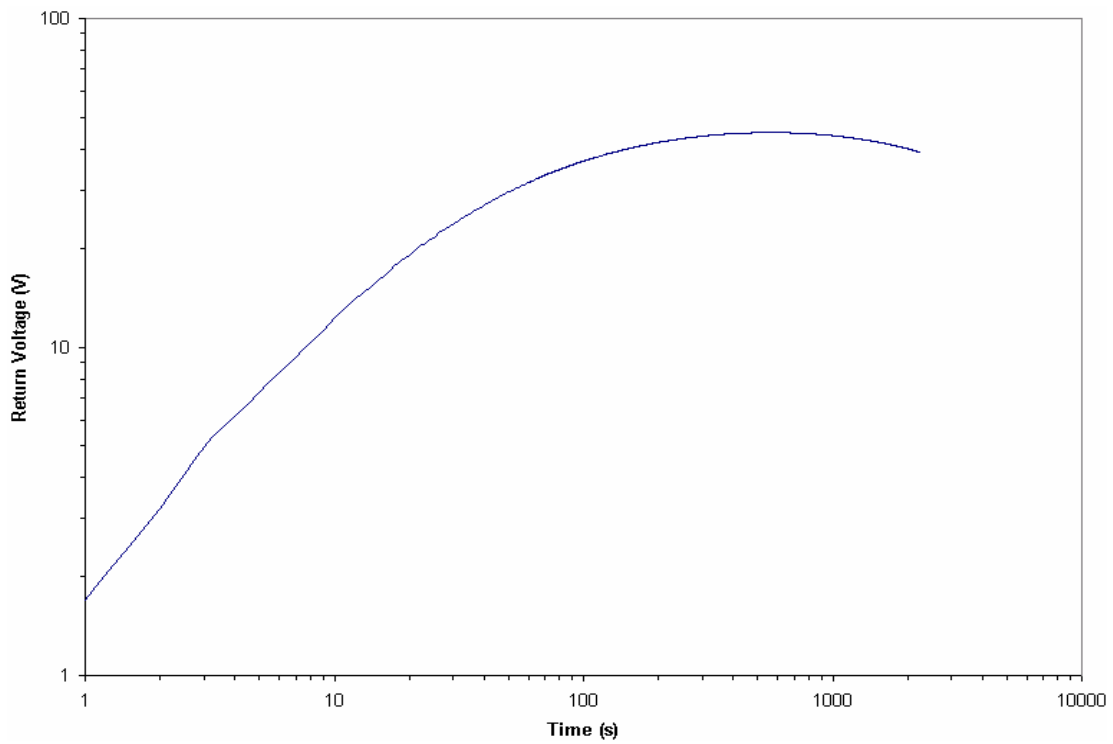


Figure 4-46
RVM response of bar T218, post-aging

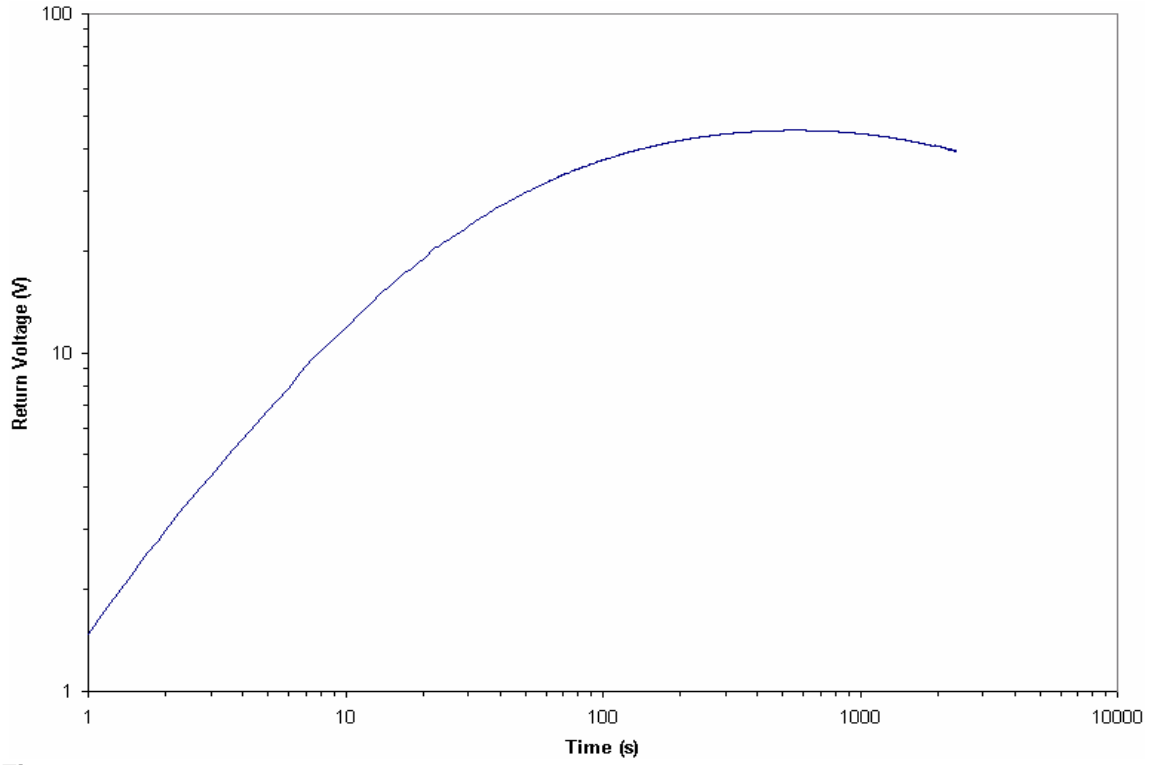


Figure 4-47
RVM response of bar T321, post-aging

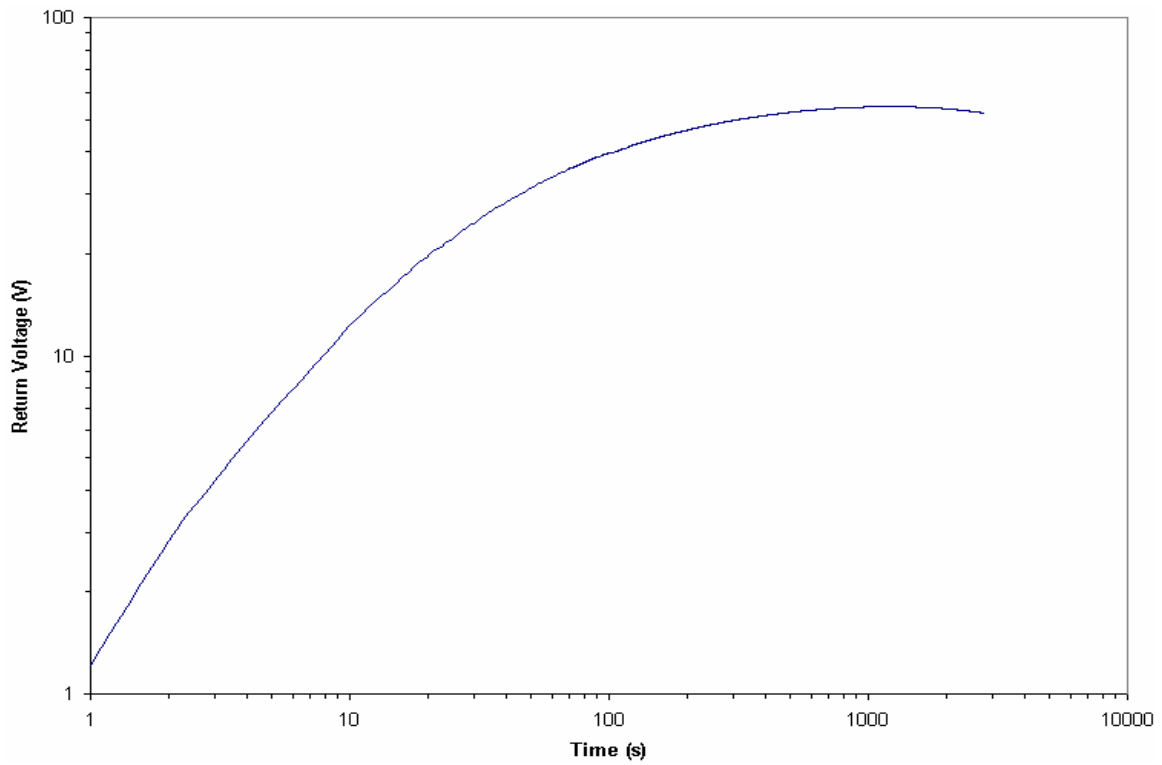


Figure 4-48
RVM response of bar B378, post-aging

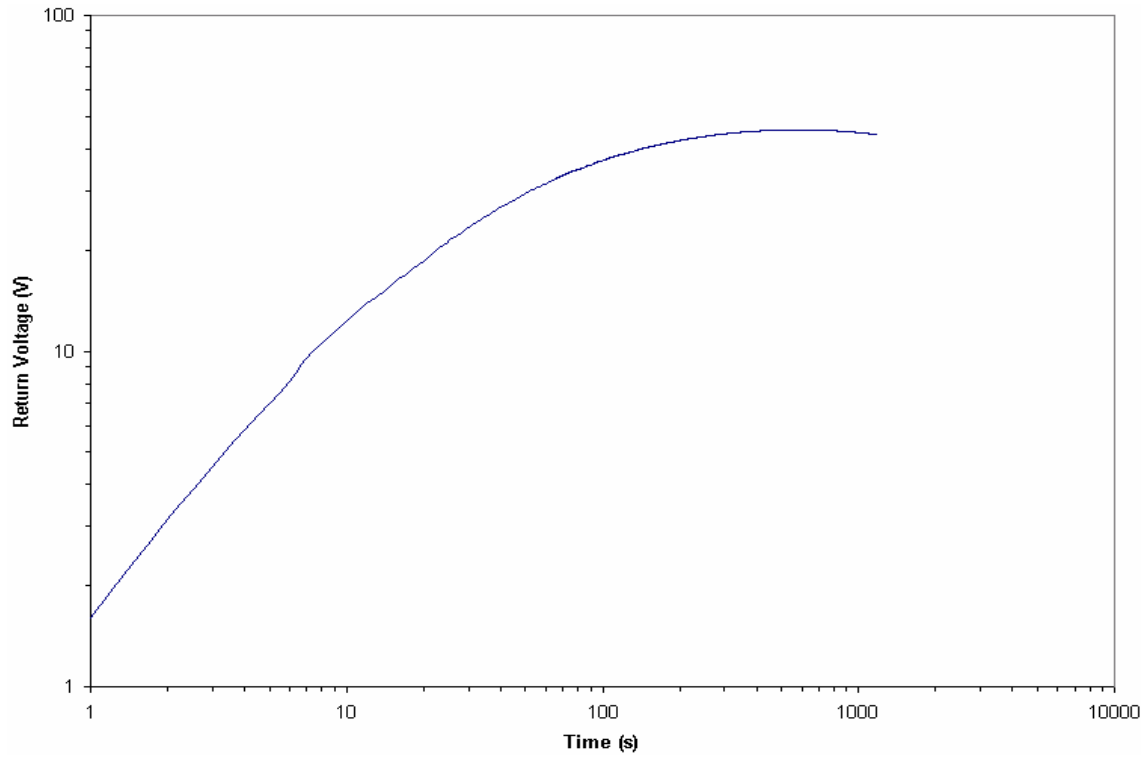


Figure 4-49
RVM response of bar T386, post-aging

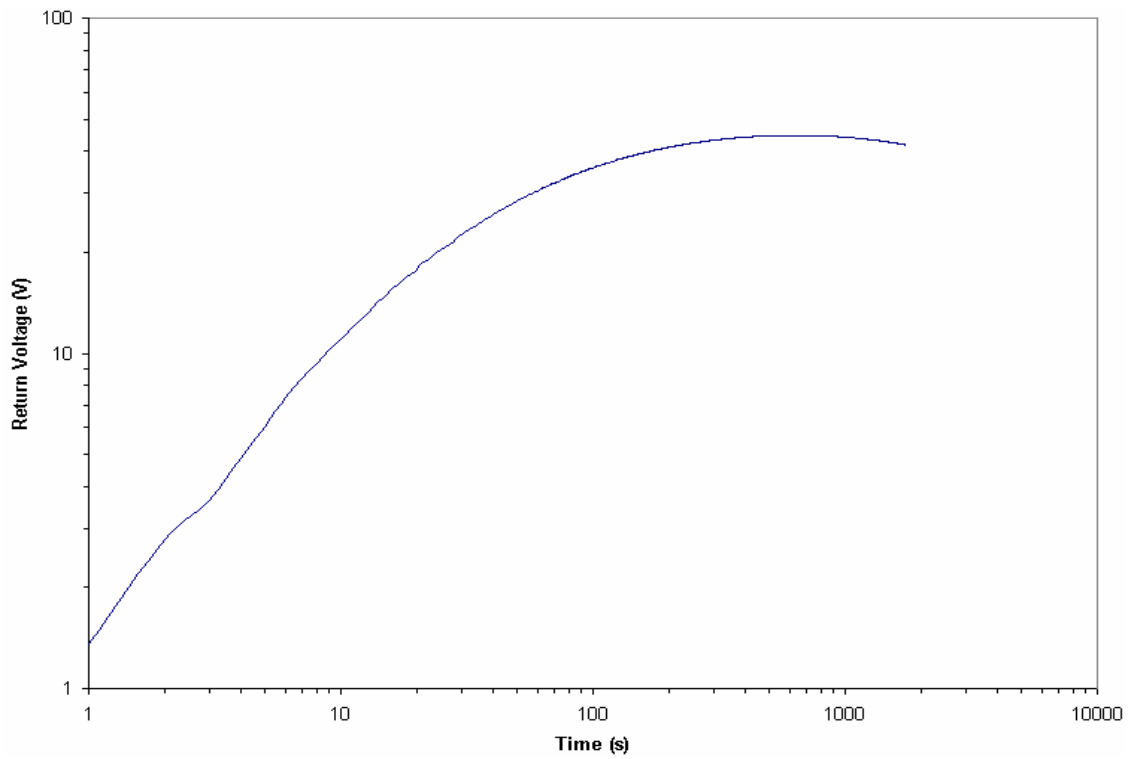


Figure 4-50
RVM response of bar B239, post-aging

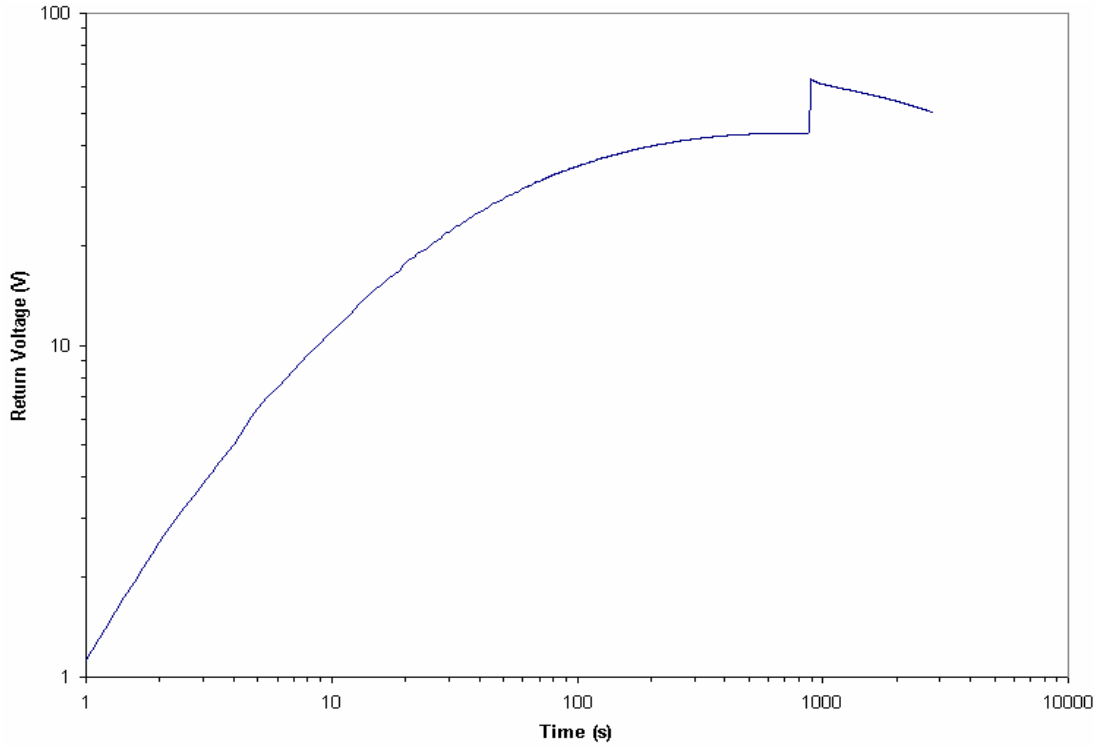


Figure 4-51
RVM response of bar B246, post-aging

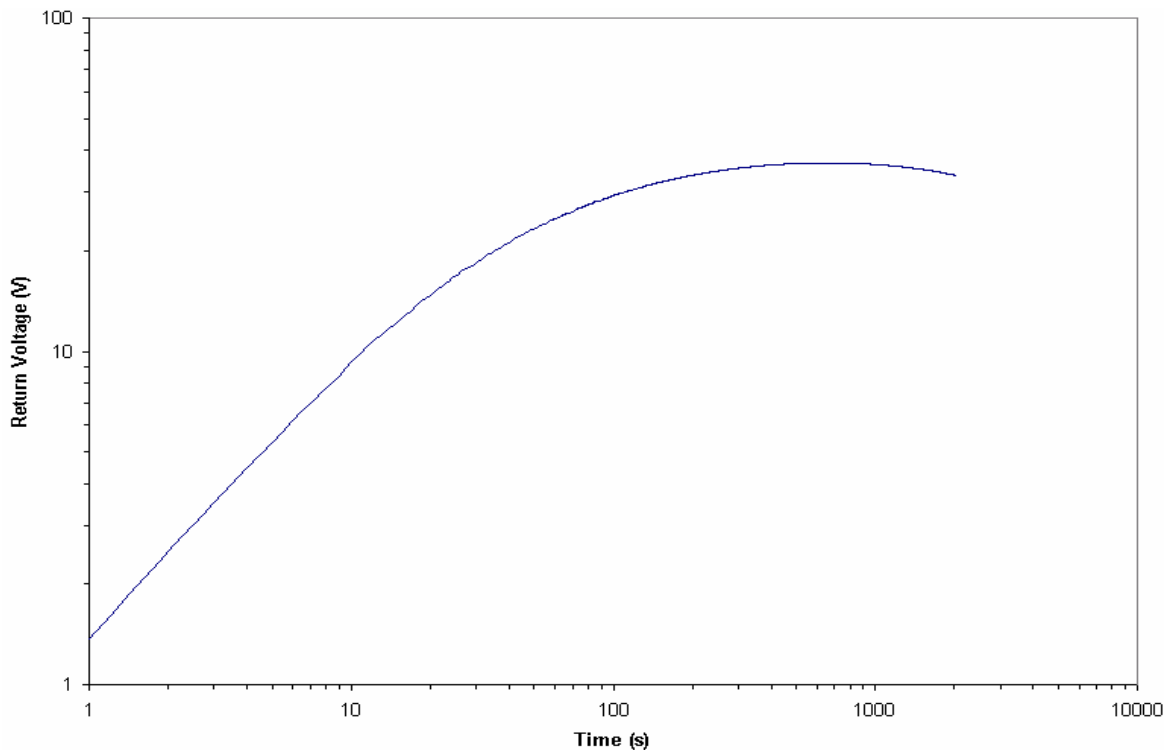


Figure 4-52
RVM response of bar T402, post-aging

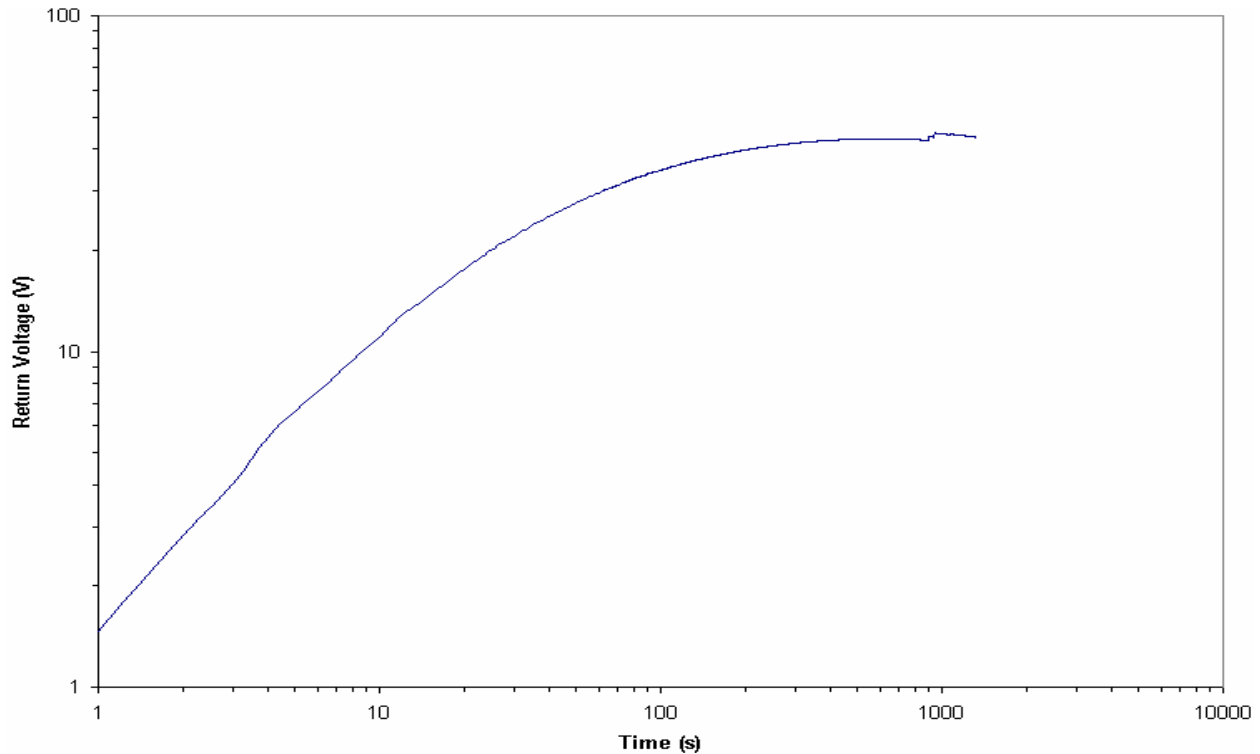


Figure 4-53
RVM response of bar B445, post-aging

There are three key features to note in the RVM characteristics. First, none of the Figures shows evidence of more than one peak, demonstrating that only one relaxation process is operative. This observation is consistent between the unaged and aged conditions. Essentially, the higher the return voltage and the shorter the time required to achieve this value, the more degraded is the insulation. Examination of Figures 4-21 through 4-42 and the data in Table 4-10 shows that the maximum return voltages, aged or unaged, are quite low. Further inspection of the data also shows that there is no consistency of the behaviour between the aged and unaged conditions, i.e., in most cases the maximum return voltage decreases after aging. Clearly, further work is required on the application of the RVM technique to stator insulation diagnostics if this method is to be considered a viable tool.

4.5 Summary of Dielectric Response Results

Examination of the low frequency dielectric spectroscopy results, Figures 4-10 through 4-31 and Table 4-8, demonstrate the following features.

1. Subsequent to aging, higher values of dissipation factor, across the frequency range of interest, are observed on bars T218, B378, T386, T402 and B445. These observations correlate well, with the exception of bar T218, with the conventional power dissipation factor data reported above.

2. Comparison of the behaviour of dissipation factor at two frequencies, 10 and 0.1 Hz, Table 4-8, shows that, on these test objects, the relationship between aging and dielectric loss is relatively linear at 0.1Hz. Analysis of the data at 10 Hz shows that in some cases the dissipation factor decreases on the aged samples.
3. Examination of the tip-up values at 10 and 0.1 Hz, Table 4-9, implies that the tip-up is frequency independent. Further, both 10 and 0.1 Hz tip-up values correlate well with the results of power frequency diagnostic tests.
4. The results also demonstrate that there is merit in taking measurements at higher voltages. Inspection of Figures 4-21 through 4-31 shows that the dielectric loss on those bars deemed to have been degraded more by artificial aging increases significantly at 10 kV and above.

Analysis of the results of RVM measurements did not obviously correlate with aging. The majority of the aged bars produced RVM characteristics which, if simple interpretation rules are used, indicate that the physical properties of the insulation have improved somewhat or not been affected at all. Such a conclusion runs contrary to all of the other electrical and physical measurements, thus further work is clearly required to understand the proper application and interpretation of this method when applied to mica-filled insulation systems.

5

CONCLUSIONS

The thermal aging of electrical insulation used in stator windings was investigated. Thermal aging was performed at a temperature of 145 C for 2700 hours on bars retrieved from a generator. To ensure significant thermal aging of the insulation, special precautions were taken to provide an unlimited supply of oxygen to the bars during accelerated aging. In addition, oxygen enriched air was used to further accelerate aging. The oxygen index of the bar materials was obtained to ensure that no safety issues arose during accelerated testing.

The thermal aging of stator coil/bar insulation was correlated to dielectric changes measured both at 60Hz and at frequencies other than 60Hz. All bars were subjected to a one minute insulation resistance test as well as standard power frequency PD, capacitance and dissipation factor tests prior to, and following, the thermal aging program. In addition, non-60Hz techniques were used. They included low frequency dielectric spectroscopy, return voltage measurement (RVM) and high voltage dc ramp.

Results of power frequency diagnostic tests demonstrated that seven bars that underwent thermal aging had suffered further degradation of the insulation system. However, the remaining three aged test objects, did not exhibit power frequency diagnostic parameters indicating that the condition of the insulation system had appreciably worsened. Examination of the low frequency dielectric spectroscopy results did not differ significantly from this finding. One explanation for this finding is that the bars had not all been aged similarly prior to artificial aging. The aging method selected employed heater plates, hence, thermal gradient problems that may be encountered when using ovens are not a factor. Thus, the differences in aging rates are likely a function of the stresses seen in-service by the bars.

Generally, all of the diagnostics employed, with one significant exception, correlated with each other and the dimensional measurements of the bars pre- and post-aging. However, the results of RVM measurements could not be interpreted and did not seem to behave linearly with aging. Such a result, although disappointing, is not altogether surprising given the paucity of public domain literature in this field. Whether or not the RVM technique is viable as a practical diagnostic for stator winding insulation, especially when tests on complete windings are contemplated, remains to be seen. Clearly, a better understanding of the test method as applied to mica-filled composites and interpretation of the results is required.

More encouraging results were obtained from low frequency dielectric spectroscopy that produced results consistent with conventional power frequency diagnostic methods. However, the purpose of using low frequency dielectric spectroscopy is to augment existing diagnostics, specifically to detect at an early stage the onset of thermal deterioration. Thus, while this low frequency technique appears promising, more work is needed to determine that the test is capable of accurately characterizing low level thermal damage.

Conclusions

Correlation, or lack thereof, between the various diagnostic tests in terms of whether or not the particular test characterized the bar as aged or unaged is summarized in Table 5-1 below. The question mark in the RVM column of Table 5-1 reflects the difficulty in interpreting the data.

Table 5-1
Summary of correlation of diagnostic results with respect to bar condition

Bar	Physical Dimension	Partial Discharge	ΔC	Tip-Up	LFDS	RVM
T5	Unaged	Unaged	Unaged	Unaged	Unaged	?
T29	Aged	Unaged	Unaged	Unaged	Unaged	?
T42	Aged	Unaged	Unaged	Unaged	Aged	?
T218	Aged	Aged	Unaged	Unaged	Aged	?
T321	Aged	Unaged	Unaged	Unaged	Aged	?
B378	Aged	Unaged	Aged	Aged	Aged	?
T386	Aged	Aged	Aged	Aged	Aged	?
B239	Aged	Unaged	Unaged	Aged	Aged	?
B246	Aged	Aged	Aged	Aged	Aged	?
T402	Aged	Aged	Aged	Aged	Aged	?
B445	Aged	Aged	Aged	Aged	Aged	?

6

FURTHER WORK

This project has demonstrated a reliable method of rapidly aging complete stator bars in a reasonable time frame. However, the results of the diagnostic tests indicate that, in some cases, the aging has progressed beyond the point at which the limits of sensitivity of diagnostic methods such as low frequency dielectric spectroscopy can be explored. Thus, some consideration may be given to refining and optimizing the aging technique used in this project.

Low frequency dielectric spectroscopy, using commercially available equipment, has been shown to be as effective in detecting the results of thermal aging as other conventional methods. Further work on understanding the application of this technique and its extension to diagnostics of complete stator windings should be seriously considered. With respect to application of the technique to complete stator windings practical issues to be considered include,

- determining appropriate test voltage levels and their implications for the requirements of the power supply
- optimizing the range of frequency to be employed
- configuration of the winding, i.e., machine frame is bonded to ground, does the test equipment need to operate ungrounded for a valid measurement.

Although the results of RVM testing were disappointing some further effort may be worthwhile to determine whether this situation could be improved by performing more fundamental work on the application of this technique to mica-filled materials.

7

REFERENCES

1. D.L. Evans, "IEEE working group report of problems with hydrogenerator thermoset stator windings, part I", IEEE Trans. Power App. & Systems, PAS-100, 1981, pp. 3284 – 91.
2. P. Mighdoll, R.P. Bloss and F. Hayashi, "Improved Motors for Utility Applications, Vol. 2: Industry Assessment Study", EPRI Report EL-2678, 1982.
3. G.C. Stone, B.K. Gupta, J.F. Lyles and H.G. Sedding, "Experience with accelerated aging tests on stator bars and coils", IEEE International Symposium on Electrical Insulation, Toronto, Canada, 1990, pp. 356 – 60.
4. IEEE Standard 1310-1995, "Recommended Practice for Thermal Cycle Testing of Form Wound Stator Bars and Coils for Large Generators", IEEE Standards Dept., Piscataway, NJ, 1995.
5. P.J. Hyde, "A wide frequency range dielectric spectrometer", Proc. IEE, vol. 117, 1970, pp. 1891 – 1901.
6. F.I. Mopsik, "A precision time domain dielectric spectrometer", Rev. Sci. Instrum., vol. 55, 1984, pp. 79 – 87.
7. J.M. Braun, R.M. Morra and H.G. Sedding, "Assessment of cable insulation by low-frequency dielectric characterization", Conference on Electrical Insulation and Dielectric Phenomena, Knoxville, TN, 1991, pp. 408 - 13.
8. J.P. Steiner, J.P. Quinlan, J.M. Braun, R.M. Morra and H.G. Sedding, "A new low frequency high voltage insulation analyzer using transient methods", Conference on Electrical Insulation and Dielectric Phenomena, Victoria, Canada, 1992, pp. 328 - 33.
9. A. Helgeson and U. Gafvert, "Dielectric response during curing of a resin-rich insulation system for rotating machines", Conference on Electrical Insulation and Dielectric Phenomena, Austin, TX, 1999, pp. 289 – 92.

Program:


Steam Turbines, Generators, and Balance-of-Plant Program

About EPRI

EPRI creates science and technology solutions for the global energy and energy services industry. U.S. electric utilities established the Electric Power Research Institute in 1973 as a nonprofit research consortium for the benefit of utility members, their customers, and society. Now known simply as EPRI, the company provides a wide range of innovative products and services to more than 1000 energy-related organizations in 40 countries. EPRI's multidisciplinary team of scientists and engineers draws on a worldwide network of technical and business expertise to help solve today's toughest energy and environmental problems.

EPRI. Electrify the World

© 2003 Electric Power Research Institute (EPRI), Inc. All rights reserved. Electric Power Research Institute and EPRI are registered service marks of the Electric Power Research Institute, Inc. EPRI. ELECTRIFY THE WORLD is a service mark of the Electric Power Research Institute, Inc.

 Printed on recycled paper in the United States of America

1009252